AQUAEXCEL

Aquaculture Infrastructures for Excellence in European Fish Research
Project number: 262336

Combination of CP & CSA
Seventh Framework Programme
Capacities

Deliverable D8.4

Title: Predictions by initial model and listing of refined simulation model modules

Due date of deliverable: M 48

Actual submission date: M 48

Start date of the project: March 1st, 2011 **Duration**: 48 months

Organisation name of lead contractor: NTNU

Revision: V2.0

Project co-funded by the European Commission within the Seventh Framework Programme (2007-2013)	
Dissemination Level	
PU Public	**X**
PP Restricted to other programme participants (including the Commission Services)	
RE Restricted to a group specified by the consortium (including the Commission Services)	
CO Confidential, only for members of the consortium (including the Commission Services)	

Table of contents

Glossary

AQUAEXCEL:	Aquaculture Infrastructures for Excellence in European Fish Research
IBM:	Individual-Based Model
DEB:	Dynamic Energy Budget

Definitions

Fish Performance:	The growth and survival of fish in a culture facility
Scale factor:	Components of the culture environment that are known to vary with the physical scale/size of the production unit and have an effect on fish performance

Summary

Objectives

This deliverable aims to provide a detailed overview of the final version of the fish model developed in WP 8 task 8.1, and further improved, adjusted and validated in task 8.4. The main aim of the model was to portray the growth of the fish in differently sized production units.

Rationale:

The work leading up to this deliverable was based on the main design choices and modelling paradigms determined in task 8.1 (see Deliverable 8.1, Annex 3). Model implementation started with a refinement and expansion of the prototype model developed in task 8.1 with additional properties and features deemed to be necessary to simulate the differences in the performance of fish reared under different scaling conditions. Further, the settings used to set up the experiments in task 8.2 were adapted into the model framework, as were the datasets on environmental factors (i.e. temperature and light) and feed delivery throughout the experimental period. This allowed the simulation of the scenarios defined by the experimental setup, and warranted comparisons between model output and experimental data from task 8.2.

While conducting the simulations, model output was continuously evaluated against experimental data. Any notable and unrealistic deviations between the two data sources was considered erroneous behaviour and investigated further. Since data from the trials using Atlantic salmon were best suited for incorporation into the model, the work in task 8.4 was mainly focused on salmon. However, the model structure is designed with sufficient flexibility to switch between different species mainly by changing parameter values.

Once a fully functional model was ready, a series of simulations based on the salmon experiments conducted in indoor tanks or marine sea-cages were conducted and used to validate and verify model functionality. Simulations based on the experiments conducted at the full scale research facilities at ACE resulted in gross SGR values over the entire period that were comparable to observed SGR values. The model overestimated the growth of the fish about halfway through the experiment, probably mainly due to an affliction by Pancreas Disease (PD) in this period, which was not represented in the model. The overall performance of the model in the comparison with the full-scale results suggests that the model was able to reproduce the main mechanisms behind salmon growth in commercial production units with acceptable precision.

Of the tank-based trials conducted in the experiments at Nofima, the model was set up to simulate the tanks with 7 and 2 m diameter (see Deliverable 8.2 for more details on the experiments). As in the experiments, the model predicted that the fish in the 7 m tank grew better than the fish in the 2 m tank, resulting in a larger end weight. This implies that our model included the components required to estimate fish performance at different physical scales. The model predicted a larger scale effect than in the experiments, as it overestimated growth to a greater degree in the 7 m tanks compared to the 2 m tanks. However, it is important to note that the performance differences observed in model output from these two cases could also partially be caused by the differences in delivery during the experiments. The model can now be used as a tool for testing hypotheses about what potential scale factors might have a significant effect on the validity of experimental results.

Teams involved:
NTNU
NOFIMA
HCMR
SINTEF
ACE

Geographical areas covered:
AQUAEXCEL geographic area

1. Introduction

1.1. Main aims

WP8 in the AQUAEXCEL project has sought to illuminate how the physical scale of production units for aquaculture impacts the performance of cultured fish and biofilters. These aspects were investigated through physical experiments (task 8.2) and the development of numerical models for estimating scaling effects in fish production units (task 8.1) and biofilters (task 8.3). In task 8.4 the aim is to evaluate to what extent the fish model developed in task 8.1 is able to predict the growth performance results obtained in the fish experiments conducted in task 8.2. Furthermore, if the correspondence between model output and experimental data is considered unsatisfactory, measures to refine the model based so that it better conforms to the data are to be sought.

Although the model framework designed in task 8.1 was intended for the simulation of both sea-bass and Atlantic salmon, main focus was kept on salmon in task 8.4 as the data from the salmon trials were more available and compatible with the model structure. The model was compared with experimental data obtained in both lab- and full-scale experiments.

Unlike fish growth, fish mortality in a production unit is difficult to describe using quantitative information from the literature. Direct causes behind mortality are often complex and will typically depend on factors such as the physical condition of the smolt when entering the facility, the genetic pedigree of the fish and stress levels associated with transport and handling. It is very difficult to obtain numerical values of how much these factors separately impact the mortality levels of the population, let alone what their combined effect will be. This will further make the derivation of a mechanistic expression of mortality suitable for implementation into a numerical model difficult. Consequently, the concept of fish performance in the present work has been limited to encompass fish growth and not mortality.

1.2. Method and approach

The mathematical model developed in task 8.1 followed a state-space based approach, meaning that the system comprised by the fish population and the conditions within the production unit are represented by a set of variables and differential equations designed to capture the system dynamics. Furthermore, the fish were simulated using Individual Based Modelling (IBM) techniques, meaning that each individual fish was treated as a separate entity in the model simulations. These design choices are more elaborately described in Deliverable 8.1 (Annex 3).

To be of practical use, a mathematical model needs to be solved either by finding the analytical solution of the equation set defining the model or by applying numerical simulation techniques. Analytical solutions are generally difficult to find if the equation set is complex, and/or is affected by stochastic effects. The present model framework possesses both these features, and thus had to be solved using numerical integration in the form of a standard forward Euler integrator with a fixed time step of 1 second. State values from the simulation are stored to disk continuously throughout a simulation, producing time series data for how the system states are changed. When simulating large populations over long periods of time, the output files would become exceedingly large if all state values of all fish were stored for each time step. The framework therefore facilitates the possibility of decimating the data by only writing the output values at time steps spaced by a specified interval (e.g. each 10^{th} sample).

The work conducted in task 8.4 was focused on collecting the relevant data and settings from the experiments conducted in task 8.2, and setting up the model to simulate the experiments based on this information. Subsequent to the simulations, model output was compared with the experimental data on fish growth, yielding a ground for evaluating the model success in reflecting the dynamics of a fish population reared in an aquaculture production facility.

2. Updated model module descriptions

2.1. Overview

The model was conceptually divided into three separate modules; the culture settings module, the environmental module and the fish module. Each of these modules was designed to handle a subset of the different aspects required to run a simulation with the model:

- Culture settings module: assembly of input parameters and calculation of derived input parameters; distribution of parameters to the other modules
- Environmental module: simulate the environmental conditions within the production unit; provide a realistic environment the fish may respond to
- Fish module: simulate the behavioural and energetic responses of the fish towards the production environment; produce behavioural, energetic and growth outputs

Figure 1 illustrates how these modules relate to each other in the total model system.

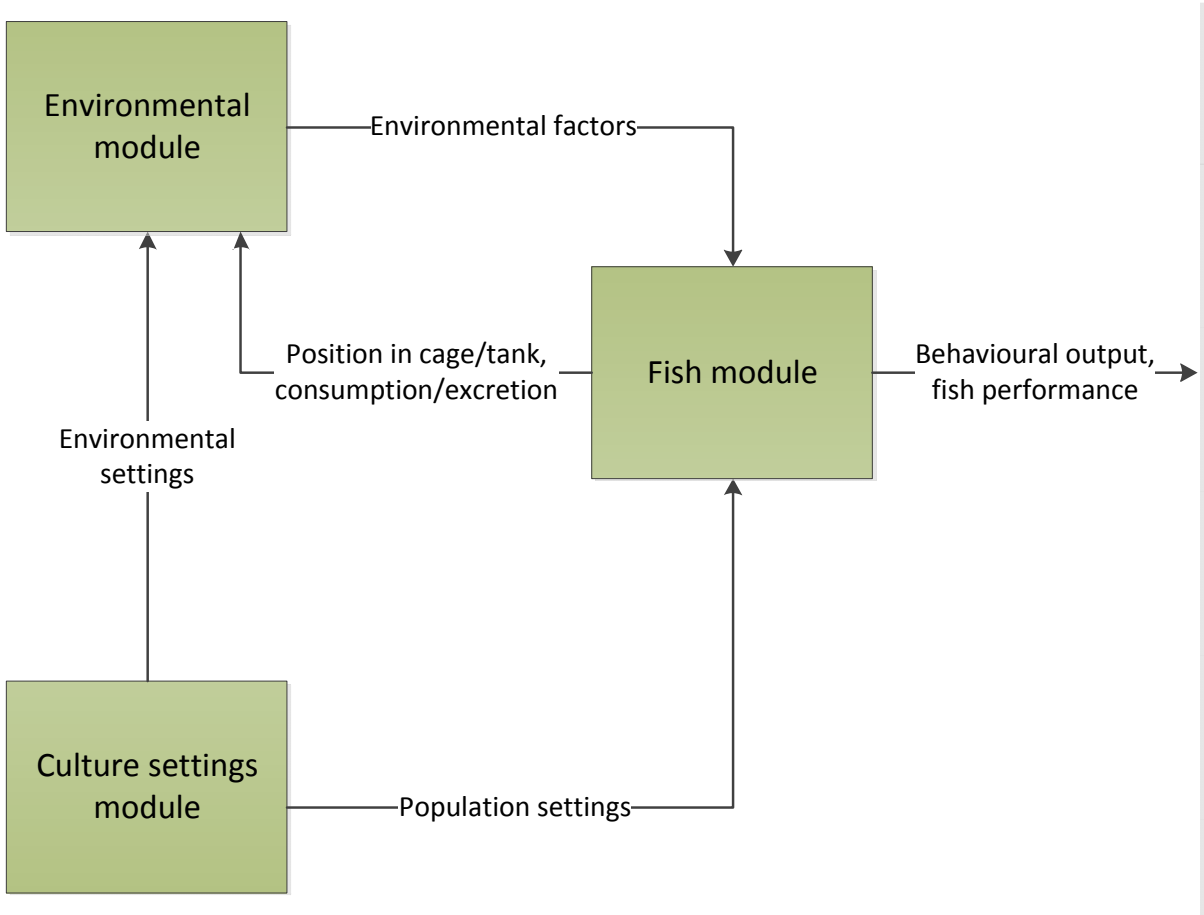

Figure 1: Description of how the three model modules interact

Although Deliverable 8.1 provided a brief overview of the general contents of the model

modules, the details of implementation were not thoroughly described. These aspects need to be outlined to warrant a sufficient background on which to discuss the implemented model and its abilities in predicting the experimental results.

2.2. Culture settings module

As explained in Deliverable 8.1 (Annex 3), the culture settings module represents the entry point to using the model, and is where the user provides the general settings and parameters required to set up a system model and start a simulation. These parameters will typically describe the start/end times of the simulation, the production unit size and location, feeding schedules and method, which environmental datasets to be used and the fish population. In the original version of the model, the parameters defining different simulation scenarios were hard-coded into the model code, and a particular simulation scenario had to be chosen upon compilation time. To ensure a higher flexibility in usage, the updated version of the model reads these parameters from XML-files during run-time, with one XML-file defining the parameters of one particular scenario. This means that a compiled and runnable version of the model can be used to simulate any scenario for which an XML-based parameter file has been defined, by specifying the name of the scenario parameter file as an inline parameter in the command to execute the model. Upon simulation initialisation, the model will then parse the XML-file and derive the input parameters necessary to start the simulation. Once the necessary parameter values have been derived, the culture settings module uses these to initialise the environmental and fish modules and create the data structures and output files necessary for the simulation to commence. Annex 2 contains an example of an input XML-file containing a complete set of scenario parameters.

In the event that the XML-file does not contain the necessary parameters, the simulation will not start but rather terminate with a notification to the user on which parameter is missing from the file. The user may then either update the XML-file with the necessary parameters, or in some cases provide these parameters explicitly as auxiliary inline commands. Available auxiliary inline commands are:

- **Time horizon**: “t_XXXX”, where XXXX denotes time horizon in seconds
- **Population size**: “n_XXXX”, where XXXX denotes number of individual fish in simulation
- **Output data decimation**: “d_XXXX”, where XXXX denotes the sample interval between each output to file (i.e. if “d_10” is provided, only every 10^{th} model output value is written to file). This option is a measure to reduce output file sizes for long simulations with large populations

If the auxiliary inline commands are used together with an input file that contains parameters for population size and time horizon, the inline values provided will override the values written in the input file. This allows the user to alter the scale of the simulation without having to modify the input file. Figure 2 contains an example of how the model may be run by providing an input file and auxiliary inline commands.

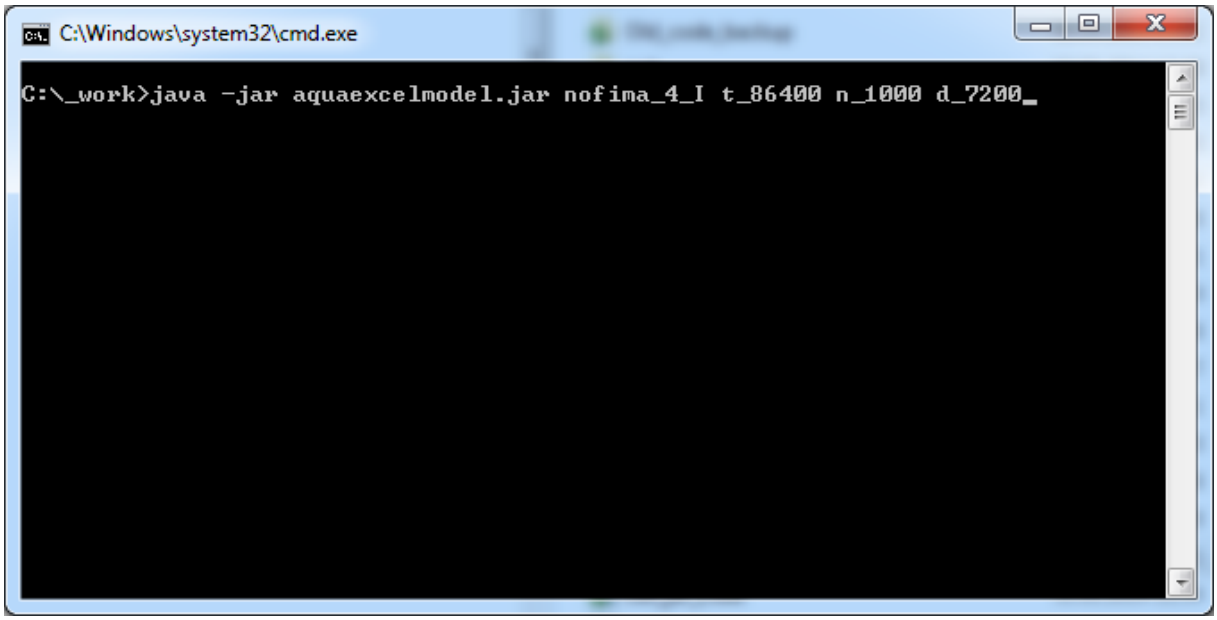

Figure 2: Example of command to run a simulation using the model. The compiled model is stored in the runnable java jar-file "aquaexcelmodel.jar", while the selected scenario is named "nofima_4_I" and describes which scenario-parameter file the model should read on startup. Inline commands "t_86400", "n_1000" and "d_7200" instructs the model to simulate 86400 sec (i.e. 24 hrs), use 1000 individual fish and write output data to file once per 2 hrs (i.e. 7200 sec) respectively.

2.3. Environmental module

As described in Deliverable 8.1 (Annex 3), the environmental module contains the models and data arrays required to present the fish with a realistic production environment. Although capable of describing an arbitrary number of different environmental features, the updated version of the module is mainly focused on defining the following factors:

- Cage/tank geometry (static)
- Temperature (dynamic)
- Light (dynamic)
- Feed (dynamic)
- Water current (dynamic)

Other features such as O_2 and CO_2 could be considered useful, but the experimental results obtained in Task 8.2 did not identify these factors as having an impact on the performance of the fish in either of the experimental trials.

Since the model is defined in 3D, the environmental model accordingly retains a global 3D definition of the environmental factors included in a simulation. However, the individual fish require a measure of the conditions local to their present position to respond to the environment. This is realised by each fish reporting their positions to the environmental model which then reciprocates with vectors describing the conditions at that location and eventual spatial gradients in these at that point. Furthermore, to ensure that the simulated fish representing a population are exposed to the same continuous environment, the environmental model is considered a shared resource between the fish. This means that each individual relates to an environmental model that is common to all fish.

Cage/tank geometry

The geometry and shape of the production unit (i.e. tank or cage) is considered constant throughout a simulation, meaning that eventual deformations are not taken into account.

Although this is a sound assumption with regards to tanks, sea-cages are known to deform both due to currents and waves, often leaving a smaller interior volume than the basic dimensions of the unit suggest (Lader et al., 2008). Over short time perspectives this could impact the performance of the fish as reductions in volume could affect the ability of the fish to attain a desirable position in the cage and also their ability to acquire the desired amount of feed. In longer simulations, however, such effects would probably even out as the main factors behind cage deformation (i.e. tidal induced currents, waves) tend to fluctuate over time.

For simplicity, production unit geometries are assumed to be either cylindrical (defined by depth and radius) or cubic (defined by side lengths and depths). The required dimensions are supplied upon simulation initialisation, and delimit the volume available for movement in the fish and also the volume for which the other environmental variables need to be specified. When a fish requests information on its proximity to the production unit confines, it is presented with the distances to the surface and cage bottom, and a 3D vector providing the distance and direction to the cage wall segment closest to its present position.

Temperature

Water temperature is a property that may vary greatly throughout a volume and with time, and is strongly dependent on the particulars of the farm locality or the tank setup. Variations in water temperature may therefore be difficult to synthesize by using a dynamic generic model. Consequently, the model developed in this project has focused on using temperature by mainly incorporating and extrapolating measured temperature values rather than having a dynamic model description. This requires that a representative dataset on temperature from the specific time period and location that is to be simulated is available. Although this may set some limits as to which scenarios may be simulated, it is very important that the temperature values used in the simulation are as realistic as possible, especially when the estimation of fish growth performance is the main aim of the simulation study. Temperature is known to be one of the most potent factors behind fish growth due to its implications for fish metabolism (Austreng et al., 1987, Koskela et al., 1997, Handeland et al., 2008).

When a fish requests the temperature at its present location, it is presented with the current temperature in Celsius, and also a 3D spatial gradient indicating the direction in which temperature increases relative to the present position.

Light

Similarly to temperature, the light levels in a production volume will vary with time and space. It is possible to set up the model with measurement data series in the same manner as for temperature. However, whereas temperature is difficult to predict using a generic model, light levels can be estimated based on time of year/day, latitude, depth and auxiliary factors such as cloud cover. The model therefore has an alternative method of initialising light conditions where a simple dynamic model developed by Kirk (1994) generates a dataset on surface light level (I_{Surf}) based on these parameters. To find corresponding light levels deeper in the water column, the surface value is subjected to the Beer-Lambert law of attenuation:

$$I_{Nat} = I_{Surf} \cdot e^{-\alpha z}$$

The value I_{Nat} thus represents the natural light level at the depth z beneath the surface, while α represents the attenuation coefficient for the passage of light through water. When z is 0, the result from equation X will equal the surface intensity (I_{Surf}). Although such dynamically obtained datasets on light may be more prone to uncertainties than when based on field measurements, they may provide a realistic estimate in cases where light data is considered unreliable due to fouling on the sensors or simply does not exist.

In addition to natural light conditions, cages and tanks may be equipped with artificial light sources, either placed above the surface or within the water column. Such sources will contribute to increase the general illumination within the cage volume, but is much more sensitive to the distance between the observation point and the source, as light is then emitted from a point in space rather than being evenly distributed across the water surface as is the case with natural light. To accommodate the presence of artificial lights, the environmental model retains a simple model of how artificial light sources affect light intensity at a given position. This model is initialised by providing the intensity of the source when seen at a distance of 1 m (I_{AS}) and the 3D position of the source. In addition, the attenuation factor determining the transmission of the source light in water (α_A) has to be supplied:

$$I_A = I_{AS} \cdot \frac{e^{\alpha_A \cdot (s-1)}}{4\pi \cdot (s-1)^2}$$

The intensity (I_A) at a specific distance (s) from an artificial light source is thus found by applying both the Beer-Lambert law of attenuation ($e^{\alpha_A \cdot (s-1)}$) and a formulation of geometric loss ($4\pi \cdot (s-1)^2$). Since I_{AS} is defined as the intensity at 1 m from the source, $s-1$ is applied rather than s in the equation.

When a fish requests the light level at a specific position, it is offered a scalar value providing the actual light level, and a 3D vector specifying the direction in which light intensity increases.

Feed

A good description of how feed is distributed in the production volume is essential for estimating the fish performance, as feed distribution together with fish movement will determine the availability of feed for the fish. In the present model framework, this is accounted for by a dynamic model of feed distribution that was originally developed to estimate the feed dispersal patterns over vertical 2D segments of a production unit (Alver et al., 2004). More recently, this model has been expanded to also handle distribution patterns in 3D volumes (Alver et al., In preparation), a feature which enabled the incorporation of the pellet distribution model into the 3D environmental definition used in the model framework. Both the 2D and 3D versions of the model have been verified and validated against experimental data to ensure that it produces realistic estimates of the feed distribution dynamics in aquaculture production units (Alver et al., 2004, Alver et al., In preparation). All elements of the model as provided by Alver et al. (In preparation) were implemented into the common model framework presented here, with the exception of the fish representation which is handled by the sub-models in the fish module.

The feed distribution model estimates both how the pellets are distributed onto the water surface by the feeding system, and how the pellets disperse within the production unit volume after having passed through the water surface. To model spatial variations in pellet concentration, the model discretises the volume of the simulated production unit into cubical cells with fixed sizes, each of which retains a specific amount of pellets (c). Pellet amounts in the cells are generally updated each simulation time step, but will require a more rapid update frequency (i.e. a time step smaller than the simulation time step) if the movement distance of the pellets per simulation time step is on the same order of magnitude as the cell size, or larger.

Feed pellets are typically delivered to aquaculture production units by feed spreaders which disperse the pellets over a percentage of the surface area. This method is in widespread use by the industry today as feed dispersal over a larger area is assumed to be beneficial for the

growth of the fish population. (Oehme et al., 2012) studied the distribution patterns produced by commercial feeding systems when varying the setup parameters of the systems. Surface distribution patterns were found to be non-uniform with respect to spreader orientation, and depend strongly on the spreader type, nozzle orientation and pneumatic airspeed (Oehme et al., 2012). To emulate such distribution patterns, the feed distribution model was equipped with a parameterised probability distribution which is a function of airspeed (v_{air}), distance from the feed spreader (d) and the rotation angle of the feed spreader relative to the forward direction of the spreader (ψ).

$$P(v_{air}, d, \psi) = \frac{1}{X_2\sqrt{2\pi}} e^{(-\frac{(\acute{d}-X_1)^2}{2X_2^2})}$$

This represents a normal distribution with mean value (X_1) and standard deviation (X_2) determined as functions of v_{air}, ψ, whether the nozzle of the feeder is tilted up or down and a set of adjustable parameters ($p_1 - p_8$). Furthermore, the variable $\acute{d}$ is found as the distance from the spreader (d) to the power of the parameter p_9, thus leading to a probability distribution parameterised by $p_1 - p_9$. Numerical optimisation was then applied to find the set of parameters ($p_1 - p_9$) leading to a distribution curve matching the feed distribution patterns observed by Oehme et al. (2012) closest in the least-squares sense. Further details on this method are outlined in Alver et al. (In preparation).

The main factors behind how pellets are distributed beneath the surface in an aquaculture production unit include feed input to the volume, feed eaten (i.e. removed) by the fish and feed transported out of the volume due to e.g. sinking and water current. These factors may be used to set up an expression for the balance of feed pellets at position x, y, z in the volume at time t:

$$\frac{\partial c}{\partial t} + v_x \frac{\partial c}{\partial x} + v_y \frac{\partial c}{\partial y} + (v_z + u_v) \frac{\partial c}{\partial z} + \kappa \left(\frac{\partial^2}{\partial^2 x} c + \frac{\partial^2}{\partial^2 y} c + \frac{\partial^2}{\partial^2 z} c \right) = u - f_I$$

The variable $c(x, y, z, t)$ is the local amount of feed, $v_x(x, y, z, t)$, $v_y(x, y, z, t)$ and $v_z(x, y, z, t)$ represent the x , y and z components of the local water current respectively, and u_v provides the sinking speed of the feed pellets. Further, $u(x, y, z, t)$ represents local feed input (due to surface feeding), while $f_I(x, y, z, t)$ represents local feed ingestion by the fish (as estimated by the behavioural sub-model in the fish module). The terms of the equation containing first order partial derivatives with respect to spatial dimensions (e.g. $\frac{\partial c}{\partial x}$) simulate advection effects, i.e. the movement of pellets due to water current and pellet sinking rate. Terms including second order partial derivatives (e.g. $\frac{\partial^2}{\partial^2 x}$) simulate diffusion effects, i.e. the tendency of the pellets to disperse over time once released into the water. The effect of the diffusion terms is controlled by the parameter κ which is called the diffusivity of the feed. To be applicable for the cell grid used in the feed distribution model, the equation needs to be discretised along the three spatial dimensions, yielding a set of discrete equations that may be used for the numerical integration. The details and results of the discretisation are given by Alver et al. (In preparation).

Alver et al. (In preparation) successfully validated the feed distribution model against experimental data. This indicates that the model may realistically estimate how the pellet distribution in an aquaculture production unit varies in time and space. The model was validated with respect to the details regarding the diffusion process, but also with respect to full model functionality through comparison with experimental data on the feed waste and consumption from an experimental cage (Figure 3).

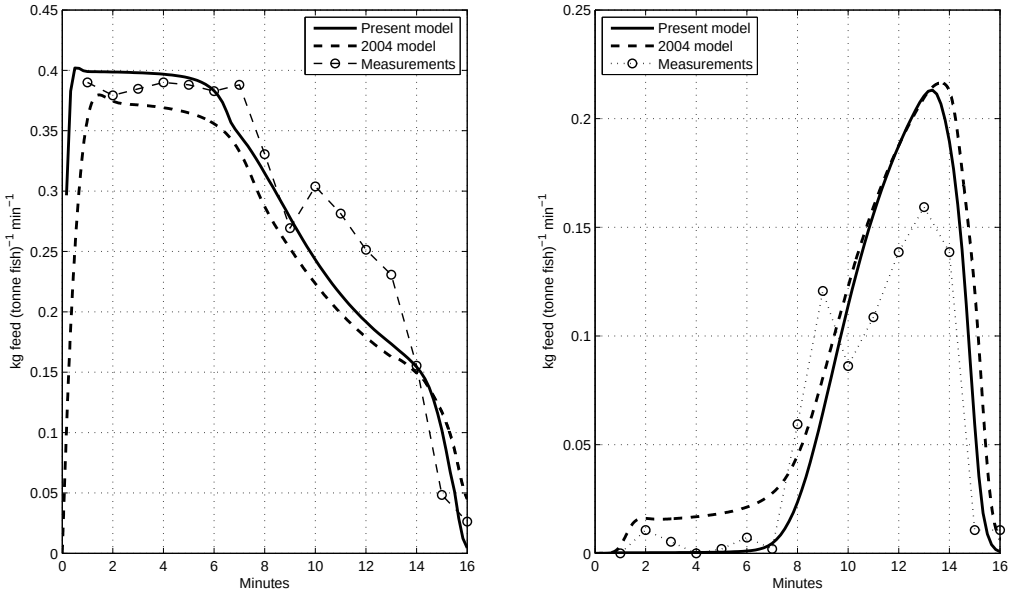

Figure 3: Measured feed waste and estimated feed intake from salmon cage (Talbot et al., 1999, circles), compared with the original pellet model (Alver et al., 2004, hatched lines) and the present 3D version of the model (Alver et al., In preparation, solid lines)

To better illustrate the three-dimensional aspect of the model, Figure 4 shows a 3D representation of the same dataset as presented in Figure 3. The distribution in 3D is rendered for six separate times during the simulation (1, 5, 10, 13, 14 and 15 min) to illustrate the development over time.

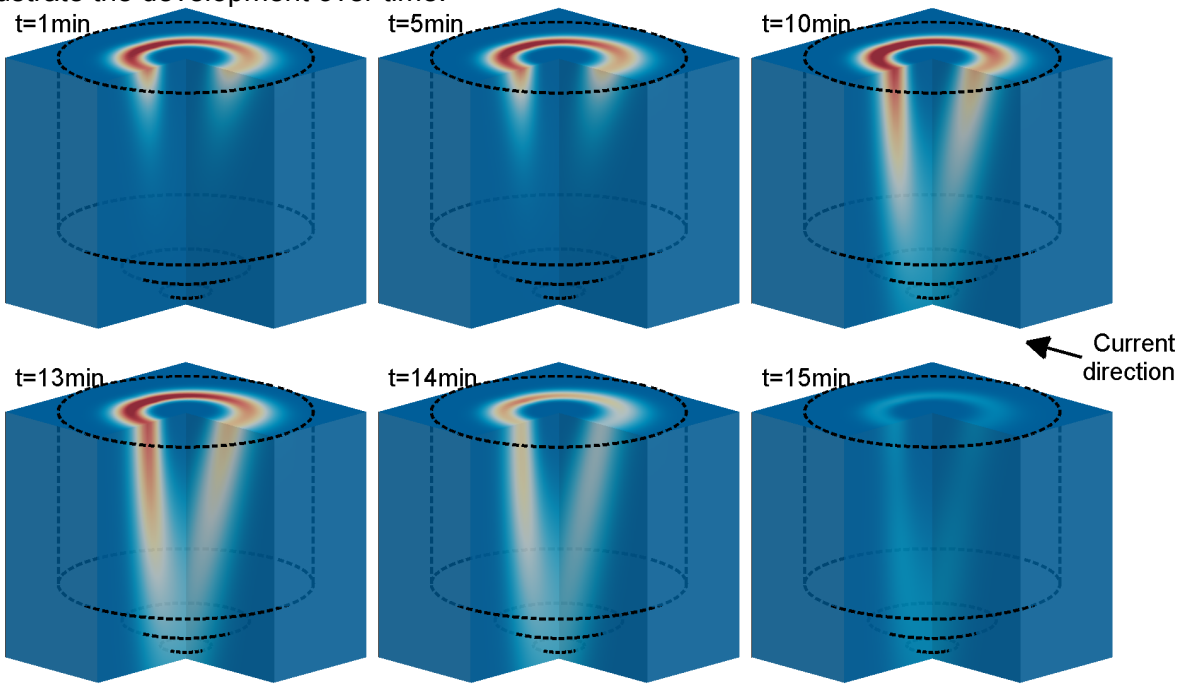

Figure 4: 3D Illustration of pellet distribution at six different times during a simulated 15 min feeding trial. The simulated feeding trial is based on the feeding scheme applied in Talbot et al. (1999). Different colours denote different feed pellet densities (red = high, blue = low), and the thick dashed lines illustrate the outline of the circular net cage used in the simulation.

Water current

Water current is an important factor in determining how the feed pellets are distributed within a production volume, and thus is essential to represent within the environmental formulation. Methods suitable for resolving the current fields within delimited volumes include approaches based on Computational Fluid Dynamics (CFD) (Harlow, 2004) and Smoothed Particle Hydrodynamics (SPH) (Monaghan, 1992). If properly set up, such methods will provide realistic estimates of the hydraulic environment within a volume, and may with some further development be adapted to also accommodate the movement of fish inside the volume. However, setting up and initialising these methods may be a time consuming and difficult task even for relatively simple geometries, and considerable computing power is often required to produce outputs with reasonably high spatial resolutions. Moreover, such methods are often based on specific integration methods that may make a model difficult to integrate with other numerical model systems. Consequently, the integration of CFD or SPH based methods into the present environmental model framework was considered outside the scope of WP8. Water flow was therefore modelled using a system of simple assumptions regarding how the patterns within a cage or a tank vary spatially and temporally.

The production volume of a net cage is only delimited by permeable netting material which allows water to pass from the ambient environment into the interior net cage volume. Flow patterns within this volume are thus mainly determined by the ambient conditions, and will typically depend strongly on tidal currents and waves. Spatial variations in currents within cages are restricted to the vertical axis in the model, keeping speed and direction at a horizontal intersection of the volume constant. Although wake effects (Løland, 1993, Blevins, 2003, Fredheim, 2005) and the presence of fish (Gansel et al., 2011) are known to impact the flow patterns within cages, this simplification was deemed to result in a sufficiently detailed current model to represent the effects of water current on the transport of pellets in the sub-surface environment. For indoor tanks, however, the situation is different. As opposed to net cages, tanks are composed by non-permeable rigid walls and typically have outlets placed at the tank bottom. The inlets in tanks are often placed along the sides of the tank, resulting in rotational current patterns within the production volume. Although tank geometry and the position and direction of water inlets largely determine the specific interior current fields in a tank (Davidson and Summerfelt, 2004), a generic trait of these patterns is that the current speed varies radially, with the highest speeds near the edge of the tank volume. To account for this, the model had to be extended to using a more advanced hydrodynamic environment when simulating the tanks.

Under the assumption that vertical speed components are small compared with horizontal components, the model was expanded with a simplified representation of horizontal variations in current speed in tanks. This was realised by mathematically approximating one of the radial current speed profiles found by (Davidson and Summerfelt, 2004), producing a tentative field of horizontal currents over a model grid representing a horizontal cross-section of the tank. The field approximates the transport of water across all cell borders defined by the grid, but may not be consistent as the discretisation of the cross section could lead to the accumulation of disappearance of water in cells. Such consistency is required by the dynamic pellet distribution model, as the net flow into and out of each model cell must add up to zero to ensure mass balance in the feed distribution. The naive tentative current field thus has to be modified to accommodate these requirements by making small adjustments to all across-border flows between cells.

In the mathematical model, water transport across cell borders is denoted by symbols u and v, $u(i,j)$ representing the flow across the border between cells $i-1, j$ and i, j and $v(i,j)$ representing the transport between cells $i, j-1$ and i, j. Consequently, the water balance for cell i, j is as follows for the unadjusted naive current field:

$$\Delta_{Orig}(i,j) = u(i,j) - u(i+1,j) + v(i,j) - v(i,j+1)$$

The terms $u(i+1,j)$ and $u(i,j+1)$ represent the fluxes between cell i, j and cells $i+1, j$ and $i, j+1$ respectively. If a cell lies along the wall of the tank, the current components are set to zero across the wall.

A term $\Delta_{Orig}(i,j)$ that deviates from zero in equation X indicates that the mass balance in cell i, j is not fully preserved, meaning that the amount of water entering the cell is not equal to the amount of water exiting the same cell. To reduce the impact of such deviations, the balance expressions for each cell is modified by local speed adjustments denoted $\delta_u(i,j)$ and $\delta_v(i,j)$ which are added to the original u and v values of cell i, j:

$$\Delta(i,j) = u(i,j) + \delta_u(i,j) - u(i+1,j) - \delta_u(i+1,j) + v(i,j) + \delta_v(i,j) - v(i,j+1) - \delta_v(i,j+1)$$

To find the sets of $\delta_u(i,j)$ and $\delta_v(i,j)$ values which lead to the best mass balance in the current field, an optimisation scheme was implemented. This scheme uses the sum of the squared balances of all cells as an object function (f_{Obj}):

$$f_{Obj} = \Sigma_{i,j}(\Delta(i,j))^2$$

A value of f_{Obj} equal to zero means that there is complete mass balance in all cells, while its value increases with increasing degree of imbalance. Through an unconstrained nonlinear optimisation method, the values of $\delta_u(i,j)$ and $\delta_v(i,j)$ which minimise the value of f_{Obj} can be found. By applying these values to the current fields derived from Davidson and Summerfelt (2004), current fields with improved mass balance are derived. Figure 5 describes the current field for a specific case, both in its initial state and after the optimisation method has been applied to adjust and improve the mass conservation between cells.

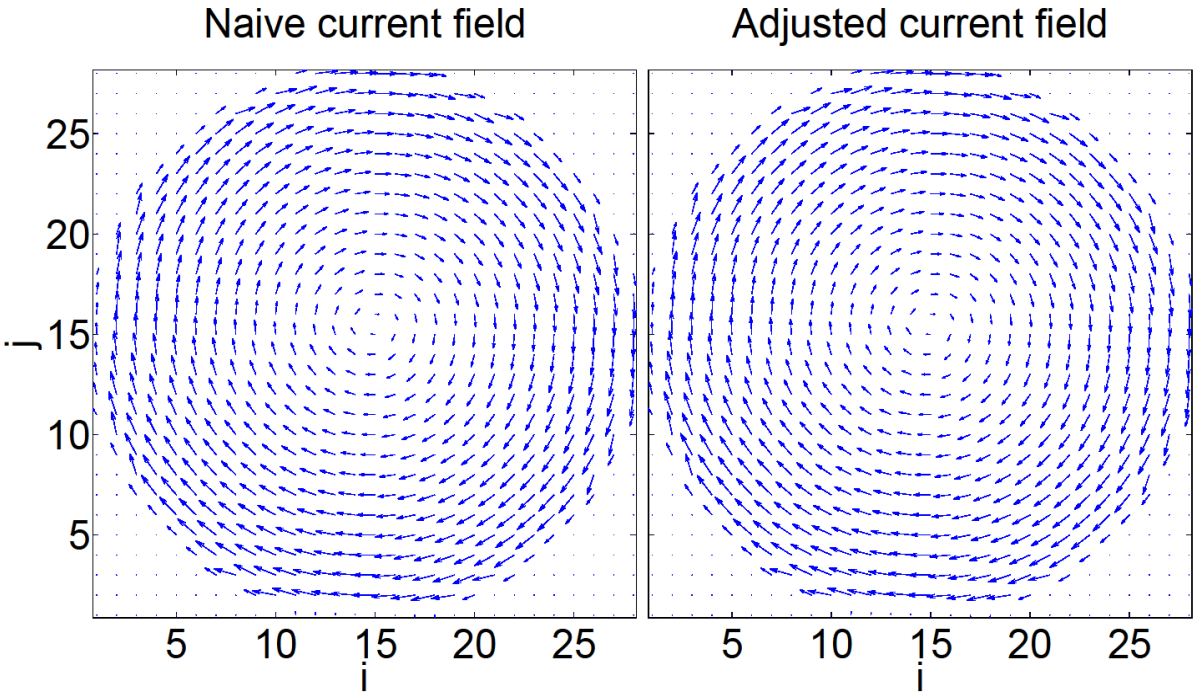

Figure 5: Differences between the initial naive current field (left) and current field adjusted through optimisation (right) for an arbitrary tank.

For simplicity, the current fields generated from (Davidson and Summerfelt, 2004) were generalised such that they could be adapted to tanks of different sizes. This allowed the use

of this method on all relevant tank geometries used in the experiments in WP 8.

Spatial conformation and interpolation

To efficiently simulate the production environment within aquaculture production units, a flexible framework for defining the spatial and temporal variations in environmental factors in a 3D volume was developed. The framework has the capability of reading in a variety of experimental data formats (i.e. measurement values) varying in space (1D, 2D or 3D) and time. This ensures that data obtained from experiments is possible to incorporate in the model irrespective of the measurement protocol.

For the fish to respond properly to the environment, it is essential that all environmental factors are defined for the entire production volume. All datasets based on measurements which do not cover the entire volume (e.g. 1D or 2D datasets) are therefore expanded through nearest value extrapolation to yield full coverage.

Furthermore, it is important that a fish will always respond to smooth environmental datasets irrespective of where the fish is located within the production volume. As the fish will usually not be located at the exact vertexes of the spatial environmental grids it is therefore necessary to utilise interpolation methods. Since the model operates in 3D this means that the environmental values for a fish at a specific place need to be derived using trilinear interpolation. This is a method which has higher computational overhead than reading a scalar value from a table. To reduce the computational cost of this operation, the model attempts to conform all datasets except the current fields and feed distribution to a common resolution. Consequently, when a fish requests the data values at its present location, only a single set of trilinear interpolation parameters need to be derived, and may be applied to all datasets that need interpolation to yield smoothness.

2.4. Fish module

Fish behaviour

The fish behaviour model was derived from previous work on modelling of salmon behaviour in sea-cages (Føre et al., 2009, Føre et al., 2013). This model aspires to simulate all individuals in a population as separate entities, and has been applied to simulation of vertical distribution patterns due to natural conditions (Føre et al., 2009) and responses toward the placement of submerged lights in the cages (Føre et al., 2013).

Simulated individuals are programmed to move in 3D, with their movement being determined by responses toward external influences (the cage/tank structure, feed, temperature, light and other individuals) and a stochastic effect. The states defining the position of a fish (r) comprises the position of the fish in Cartesian coordinates (x, y and z) and the pitch (θ) and yaw (ψ) angles of orientation.

The total behavioural response for a fish is computed by first finding the reference movement vector ($\dot{r}_{ref}$) as a weighted sum of the specific responses toward the different influences:

$$\dot{r}_{ref} = \tau \cdot \dot{r}_{prev} + (1-\tau) \cdot (k_C v_C + k_F v_F + k_T v_T + k_L v_L + k_{SO} v_{SO} + k_{ST} v_{ST})$$

The v-arrays (i.e. $v_C, v_F, v_T, v_L, v_{SO}$ and v_{ST}) in this equation denote the specific 3D-responses caused by the tank/cage (subscript *C*), feed (*F*), temperature (*T*), light (*L*), other individuals (*SO*) and stochastic effects (*ST*). Correspondingly, the 3D-responses are associated with weighting factors (i.e. $k_C, k_F, k_T, k_L, k_{SO}$ and k_{ST}) whose values are determined through a hierarchical scheme based on the assumed importance and priority of these factors for the

fish. The hierarchy scheme also maintains a finite "quota" for movement, ensuring that the total sum of all weighting factors never exceeds 1. This prevents the modelled fish from exhibiting unrealistically high swimming speeds (see Føre et al., 2009, Føre et al., 2013 for more details on the hierarchical determination of weighting factors). The parameter τ determines how much the velocity vector of the fish is allowed to change between time steps in a simulation. For example, a τ set to 1 would result in that $\dot{r}_{ref}$ is kept identical to the velocity vector from the previous time step ($\dot{r}_{prev}$) throughout a simulation. This would make the fish swim in a straight line, never changing its course. Decreasing τ will increase the impact of responses toward the present external influences and stochastic effects on the fish movement.

While specific response patterns toward the cage/tank structure, temperature, light and other individuals are described by Føre et al. (2009, 2013), the responses toward feed had to be adjusted as the model was merged with the pellet distribution model. In the original version of the behavioural model, feed was defined as an unlimited supply delivered over a pre-defined area on the surface. The behaviours of the fish were largely governed by a set of probability values for detecting feed (p_d), capturing feed (p_c) and feeling hungry (p_a), with p_d and p_c computed as functions of distance to the feeding area and p_a a function of relative stomach fullness. Based on these probabilities, the fish then responded by either disregarding the feed, approaching the feed or trying to ingest feed (Føre et al., 2009). This general setup and sequence of events was retained in the implementation in the present model framework, though with altered values for p_d, p_c and p_a. The new expressions for the two former of these were based on information received from the pellet distribution model:

$$p_d = \frac{c_{Tot}}{(1 + c_{Tot})}$$

$$p_c = \frac{\rho_f}{(1 + \rho_f)}$$

Parameters c_{Tot} and ρ_f are obtained from the feed distribution model and represent the total amount of feed in the cage (g) and the density of feed (g m^{-3}) at the present location of the fish respectively. The primary motive behind these alterations was to connect the feeding aspect of the behavioural model with the pellet model. However, these changes also accommodated a set of assumptions about how salmon feed, the first of which was that the probability of detecting the presence of feed (p_d) should depend on the total amount of feed (c_{Tot}) but be independent of the present location of the fish. This is reasonable as a certain amount of feed delivered to a commercial cage would lead to both aural cues (from the feeding system) and visual cues (other fish displaying feeding behaviour) that would be perceptive from any location within the cage. The probability of capturing a pellet (p_c) however, depends strongly on the position of the fish in depending on the local density (ρ_f) of pellets. This is a necessary dependency, as a fish can only ingest pellets that are in its vicinity, and may be a likely approximation as the likelihood of capturing a pellet would increase with the local feed density.

The final probability function (p_a) was set up to depend on input from the energetic model:

$$p_a = 1 - G_{Rel}{}^2$$

Where:

$$G_{Rel} = \frac{G}{G_{Max}}$$

$$G_{Max} = 0.009 \cdot V$$

The variables G and V are state variables in the energetic model which reflect the present gut

contents and structural volume of the fish, respectively. In the original model, max gut volume (G_{Max}) depended on the wet weight of the fish, but preliminary simulations using the present framework indicated that this formulation resulted in unrealistically large stomach volumes as the fish grew larger. Furthermore, since the wet weight of a fish comprises both structural mass and the mass of the reserves of the fish, it was deemed a more realistic path to use an expression for max stomach volume which adhered directly to the structural volume (V) of the fish. The expression for relative gut volume (G_{Rel}) was kept unchanged in the present model. Initial simulations revealed that the original expression for p_a as obtained from Olsen and Balchen (1992) produced too low appetite values, especially toward the latter parts of long time-scale simulations. A simpler expression was therefore adapted, which ensured that appetite would stay high for intermediate degrees of gut fullness, rather than decreasing rapidly as G_{Rel} increased above 0.5 as in the original model.

In cases where the hydraulic dynamics within the production unit is important to include in the simulation, the expression for $\dot{r}_{ref}$ is expanded to also include a response toward the water current at the present position of the fish (v_{WC}):

$$\dot{r}_{ref} = \tau \cdot \dot{r}_{prev} + (1 - \tau) \cdot (v_{aggr} + v_{WC})$$

The term v_{aggr} in this equation represents the value of the response toward all other external factors and stochastic effects. Unlike the responses to the factors contained in v_{aggr} (i.e. v_C to v_{ST}), v_{WC} is not associated with a weighting factor, by the assumption that the fish will need to compensate for water current irrespective of their other behavioural decisions.

When travelling with the current, the fish will not need (or be able) to countermand the effects of the current, thus the first step in finding the value of v_{WC} is to identify the angle (α) between the current movement direction of the fish and the water current direction. An $\alpha < \frac{\pi}{2}$ would thus result in a v_{WC} with zero magnitude:

$$v_{WC} = \begin{cases} -\frac{V_c}{|V_c|} \cdot M_{WC}, & If\ \alpha \geq \frac{\pi}{2} \\ [0 \quad 0 \quad 0], & Otherwise \end{cases}$$

The term V_c denotes the current velocity vector at the present location of the fish in Cartesian x, y, z coordinates, while the parameter M_{WC} is found by subtracting the component of the amplitude of v_{aggr} that opposes the current velocity vector from the amplitude of the current velocity ($|V_c|$). Consequently, in cases where the current speed is higher than the movement of the fish opposing the current v_{WC} will compensate for this difference, preventing the fish from being forced backward by the current. An exception from this will arise when the current speed is higher than the maximum movement speed of the fish.

Although $\dot{r}_{ref}$ represents the movement direction and magnitude of the fish as motivated by external and stochastic effects, the translational movement of the simulated fish is restricted to being along the longitudinal axis of the fish body. This means that the fish need to rotate their bodies along the lateral and vertical axes to attain arbitrary positions in the cage/tank. Mathematically this is realised by rotating $\dot{r}_{ref}$ to the local coordinate system defined by the present orientation of the fish (given by the orientation angles ψ and θ). The values along the y and z axes in the fish-local coordinate system in the resulting rotated array are then set to zero, whereas the value along the local x-axis is multiplied with the characteristic swimming velocity of the fish. Based on earlier experimental results, the characteristic swimming speed was set to 0.5481± 0.0591 body lengths s^{-1} (Dempster et al., 2008), effectually scaling the movement of the fish to a realistic range of speeds in m s^{-1}. The resulting array is then rotated back to the inertial coordinate system and used as the behavioural component ($\dot{r}_{beh}$) of the position derivative ($\dot{r}$) of the fish.

The position derivative ($\dot{r}$) used to update the position of a fish (r) is then derived by adding the current velocity vector (V_c) added to $\dot{r}_{beh}$, thus subjecting the movement of the fish to the physical effect of the water flow:

$$\dot{r} = \dot{r}_{beh} + V_c$$

Fish energetics

The energetic dynamics of the fish is modelled using the principle of Dynamic Energy Budget (DEB) modelling, which is based on a set of assumptions on how organisms of all types (e.g. animals, plants, bacteria) acquire, store and utilise energy (Kooijman, 2000, van der Meer, 2006). Although plants require more advanced model formulations, most organisms may be portrayed using DEB models which distribute the ingested energy between a single reserve for energy storage, structural growth, maintenance costs and reproductive costs. Such models have been developed for a range of aquatic organisms including adult fish (e.g. Pecquerie et al., 2009), bivalves (e.g. van der Veer et al., 2006, Rosland et al., 2009, Handå et al., 2011), zooplankton (e.g. Alver et al., 2006, Peeters et al., 2010) and fish larvae (e.g. Alver et al., 2007). Figure 6 illustrates the outline and energy flow of a typical DEB model formulation.

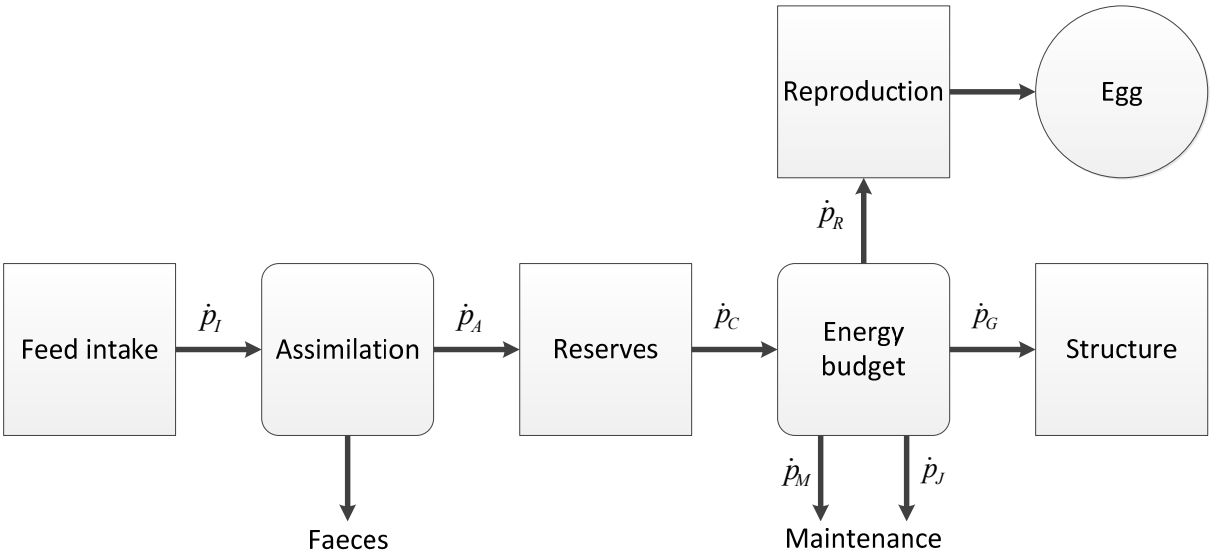

Figure 6: Outline of the basic DEB model structure which is applicable to most organism types. Arrows denote energy flow between the different compartments (inspired by Figure 1 in Alver et al., 2006).

DEB model formulations portraying the energy flow in animals of different species are most often obtained solely by adapting the parameters governing the distribution rates ($\dot{p}$-values) between the different compartments in the generic model structure (Figure 6). Other cases may however require some structural changes to the generic formulation to capture the energetic dynamics. In finfish aquaculture, it is generally an aim to prevent the fish from maturing as the maturation process will channel energy flow into gamete production, thus affecting meat quality and reducing growth (Aksnes et al., 1986). Consequently, when formulating a DEB model for farmed fish, the reproduction and egg deposits in Figure 6 may often be excluded from the model.

The energetic model chosen for the present framework was a DEB-formulation for farmed

Atlantic salmon developed by Marafioti et al. (2012). Structurally, this model resembles the model for cod larvae presented by Alver et al. (2007), omitting the reproductive elements of generic DEB formulations. To represent the gut contents of the fish, a state variable for this is added, and the energy input to the DEB model is represented by the gut evacuation rate, modulated by a feed assimilation efficiency parameter. Suitable parameters for representing the energetic dynamics of salmon were derived by adapting the model to experimental data.

The state variables of the DEB model utilized here are the structural volume V (cm^3), the energy reserve E (J) and the gut contents G (J), and these are governed by the following equations:

$$\frac{dV}{dt} = \frac{\kappa \dot{p}_C - [\dot{p}_M] C_T V}{[E_G]}$$

$$\frac{dE}{dt} = \dot{p}_A - \dot{p}_C$$

$$\frac{dG}{dt} = \dot{p}_I - a_1 T^{a_2} G$$

where

$$\dot{p}_A = k_{as} a_1 T^{a_2} G$$

$$\dot{p}_C = \frac{[E]([E_G]\dot{v} C_T V^{2/3} + [\dot{p}_M] C_T V)}{[E_G] + [E]\kappa}$$

$$C_T = \frac{\exp(\frac{T_A}{T_1} - \frac{T_A}{T})}{1 + \exp\left(\frac{T_{AL}}{T} - \frac{T_{AL}}{T_L}\right) + \exp(\frac{T_{AH}}{T_H} - \frac{T_{AH}}{T})}$$

Where $[E] = E/V$. The model parameters are listed in the following table:

Variable	*Description*	*Value*
a_1	Gut evacuation parameter	0.45
a_2	Gut evacuation parameter	0.76
$[E_G]$	Volume specific cost of growth	1900 J cm^{-3}
k_{as}	Assimilated fraction of ingested feed	0.7
κ	Energy partitioning parameter	0.7
$[\dot{p}_M]$	Volume specific maintenance rate	145 J cm^{-3}
$\dot{v}$	Energy conductance	0.21 cm d^{-1}
T_1	Temperature dependence parameter	285 K
T_A	Temperature dependence parameter	7000 K
T_{AH}	Temperature dependence parameter	10000 K
T_{AL}	Temperature dependence parameter	30000 K
T_H	Temperature dependence parameter	289 K
T_L	Temperature dependence parameter	283 K

The values of C_T given by temperature dependence parameters are shown in Figure 7.

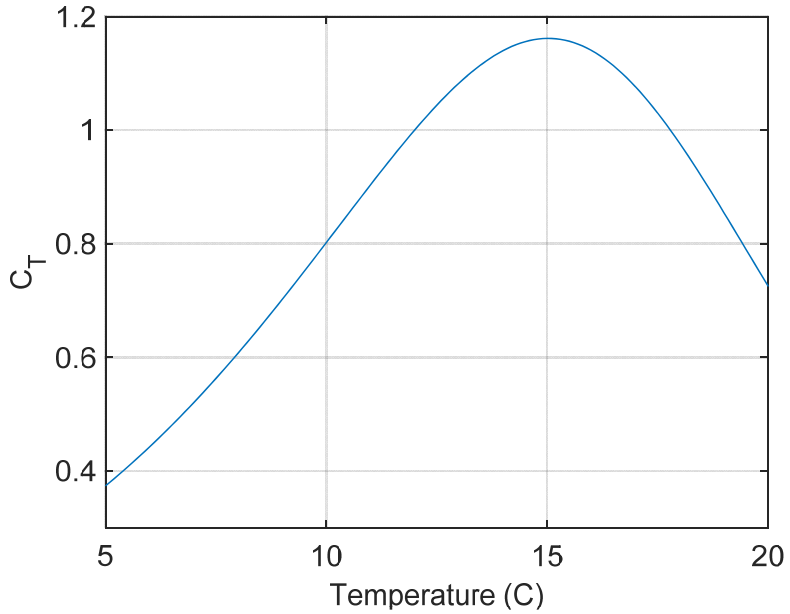

Figure 7: Temperature factor C_T, as determined by the temperature dependence parameters used.

2.5. Total system model, interaction between modules and scheduling

By properly interconnecting the model modules, a full system model is acquired. The interconnection requires transfer of information between the model modules as outlined in Figure 8.

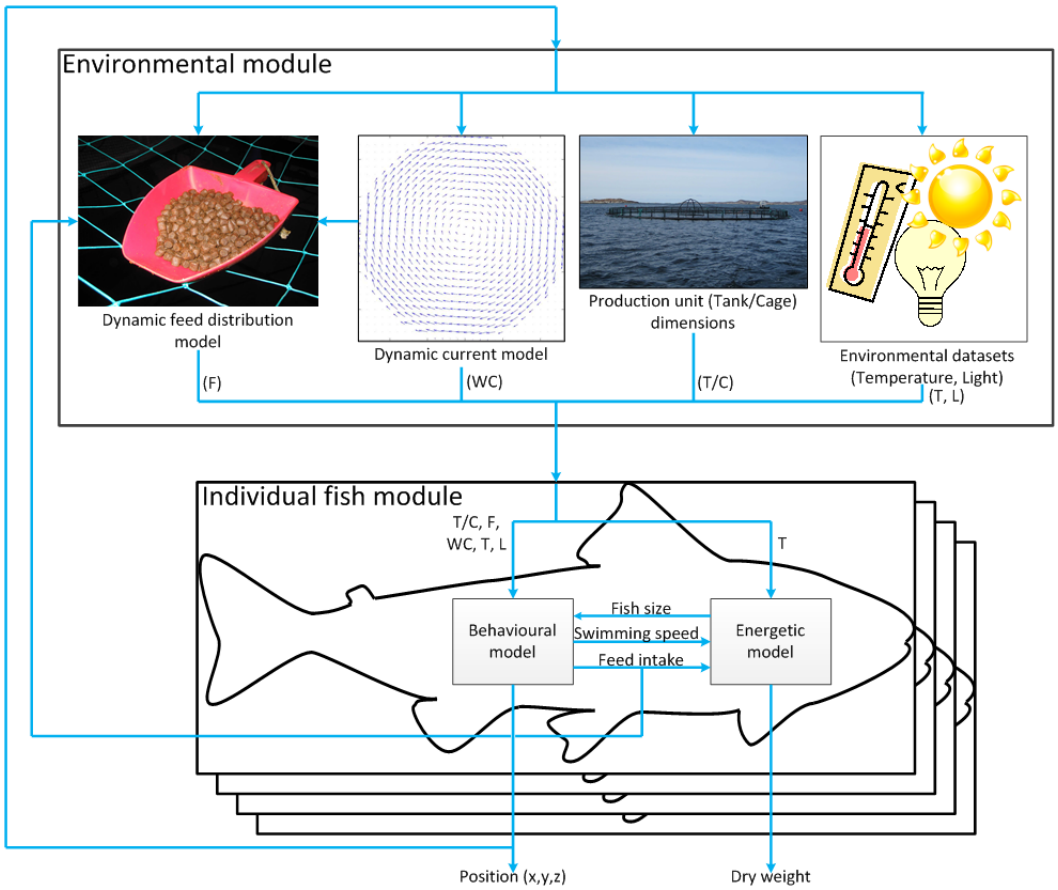

Figure 8: Interconnections between the environmental module and the individual fish module, illustrating the interplay between the environmental, behavioural and energetic submodels in the framework. Blue arrows denote transfer of information.

Based on the present position of an individual fish, the environmental module derives appropriate return values from all environmental submodels (F, WC, T/C, T, L) and returns these to the fish module. These inputs are then forwarded to the behavioural and energetic submodels within the fish module, which through interactions between themselves and internal computations produce updated values of fish position and dry weight.

To ensure a valid result in the numerical integration of the total system model, the events occurring in a time step need to be executed in a specific order (Figure 9).

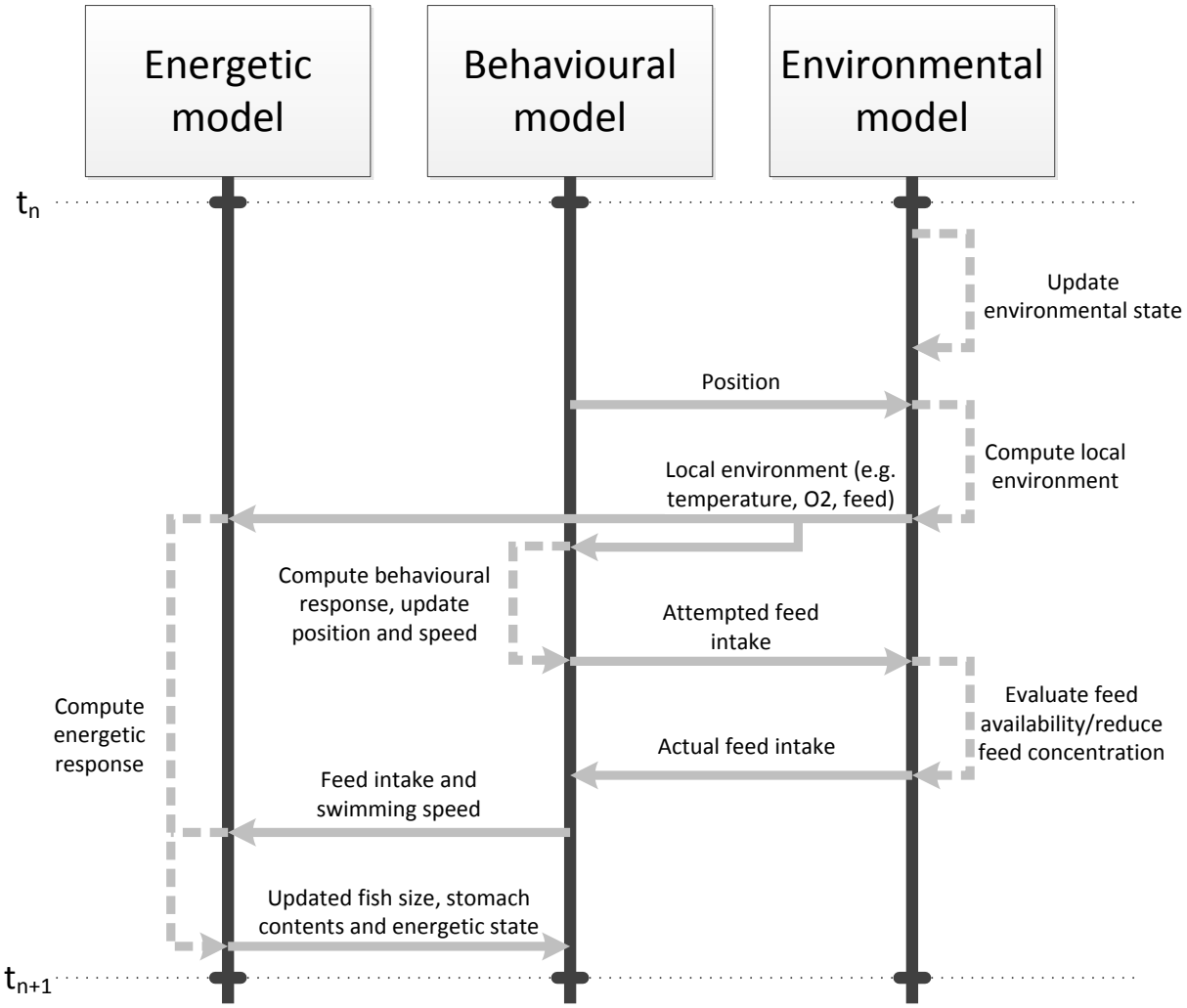

Figure 9: Sequence diagram describing the sequence of events occurring in the time step from t_n to t_{n+1} for a single individual. Vertical black lines represent time lines of the energetic, behavioural and environmental sub-models, solid arrows denote exchange of information, while dashed arrows mark processes occurring internally within a sub-model.

The first event that needs occur at each time step cycle is that the environmental model updates its present state arrays. This is done by integrating the dynamic models for current and feed, and by iterating through the datasets for physical environmental factors (e.g. temperature, light). Each fish will then report their present position to the environmental model, which reciprocates with computing the local environment at the present position of the fish and returns these to the fish. The fish will then compute its behavioural response toward the local conditions, both in terms of movement and feed intake. If feed is presently delivered to the cage, and the fish accordingly desires to ingest feed pellets, the amount of desired feed is returned to the environmental model. The environmental model then evaluates whether there is sufficient feed in the vicinity of the fish to cover the amount requested by the fish. If local feed exceeds the requested amount, the requested amount is reported back to the fish. Otherwise, the environmental model will return the maximum available feed at the present location of the fish. This return value represents the actual feed intake of the fish, and the local feed concentration is reduced by the same amount to ensure that the amount returned to the fish is removed from the feed distribution. The behavioural model then reports the actual feed intake along with the swimming speed to the energetic model which then computes the energetic response of the fish. Updated fish size, stomach contents and energetic states are then reported back to the behavioural model, concluding the events for time step from t_n to t_{n+1}.

3. Simulation results

To fulfil the aims of task 8.4, the model was set up to simulate the experiments conducted in task 8.2. This included both full scale experiments conducted at a commercial farming site and lab scale experiments performed in a range of differently sized tanks. These experimental series were executed between March and October 2012 and aimed at reaching a mean end wet weight of 750 g from an initial individual mean weight of 72.1 ± SD 2.8 g. The main purpose of the experiments was to evaluate whether the physical scale of a production unit affects fish performance, thus fish from the exact same genetic strain and cohort were used in the fish farm and tank experiments. Furthermore, the tank experiments were designed to accommodate the same feeding regime and temperatures in the tanks as in the sea-cages to enable a more detailed comparison between the full- and lab-scales. The experimental setups and results from task 8.2 are more elaborately explained in Deliverable 8.2.

3.1. Comparison with full scale experiment

Setup of physical experiment

The full scale experiments were conducted in an experimental fish farm run by AquaCulture Engineering AS (ACE) at Korsneset in mid-Norway. Three commercial size net-cages (circumference 120 m, depth 12 m) were each stocked with 120.000 individual fish. Feed input to each of the cages was registered throughout the experimental period, keeping track of amounts, start time and duration of each feeding period. Temperature and light was logged each 10^{th} minute at ten depths between 0.5 and 15 m, providing coverage of the eligible depths in the cage (0-12 m). Furthermore, average fish size was manually sampled in all cages during lice counts throughout the experimental period. In addition, cages 6 and 7 featured VAKI biomass frame systems, providing a more continuous and detailed sampling of average size. At the final day in the experiment, 160 fish were retrieved from each cage and measured accurately to obtain a more detailed final estimate on fish size.

Experimental results

As expected from such experiments, the mean individual wet weight in all three cages increased throughout the experimental period, with the mean weights in cages 5, 6 and 7 ending up at 878, 849 and 739 g respectively (Figure 10). The cages also exhibited moderate cumulative mortalities, with 9% in cage 5, 6.5% in cage 6 and 7.5% in cage 7.

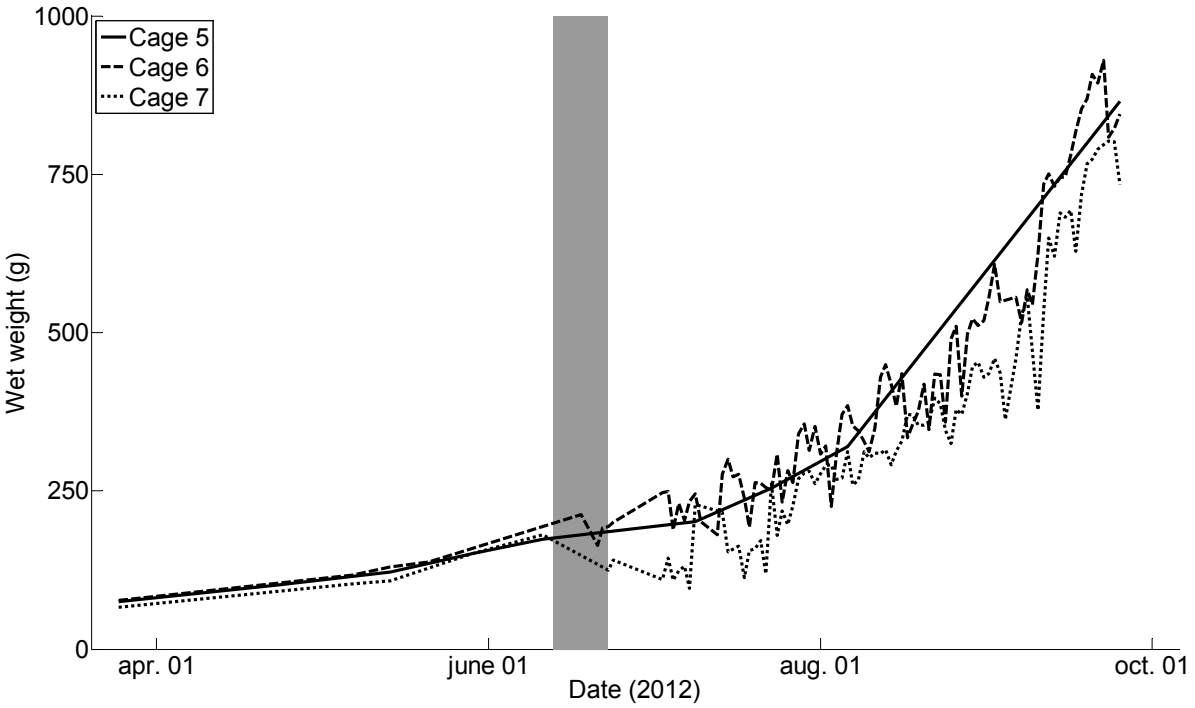

Figure 10: Growth trajectories from the three cages used in the full-scale experiments. Solid, dashed and dotted lines represent the three different cages, with the horizontal axis giving date and the vertical axis denoting the average individual wet weight in g. The high sampling rate of the VAKI frames give more rapid variations in the weight estimates for cages 6 and 7 . The grey vertical bar in the middle of the period marks the period in which PD was found at the farm.

Midway through the experiment, Pancreas Disease (PD) broke out in all three cages (Figure 10). PD is known to have negative impacts on the survival and growth of salmon (McVicar, 1987, McLoughlin et al., 2002, McLoughlin and Graham, 2007), thus it is likely that the performance of the fish was reduced by disease in the last months of the study. This is also visible in the growth trajectories in that their shapes were slightly altered after the outbreak (Figure 10).

Temperature ranged between 4.8 and 19.1 °C during the experiments, with a mean value of 11.5 °C for the entire experimental period (Figure 11). As expected, the first months of the experiment (May-July) featured generally lower temperatures (min: 4.8 °C, max: 17.7 °C, mean: 10.1 °C) than the remaining experimental period (min: 8.7 °C, max: 19.1 °C, mean: 12.9 °C). Vertical variations in temperature were higher in the early stages of the experiment than toward the end (Figure 11). Dissolved oxygen levels never went beneath 70% during the experiments and generally stayed at high saturation levels (up to 100%).

See Deliverable 8.2 for more details and discussion of these results.

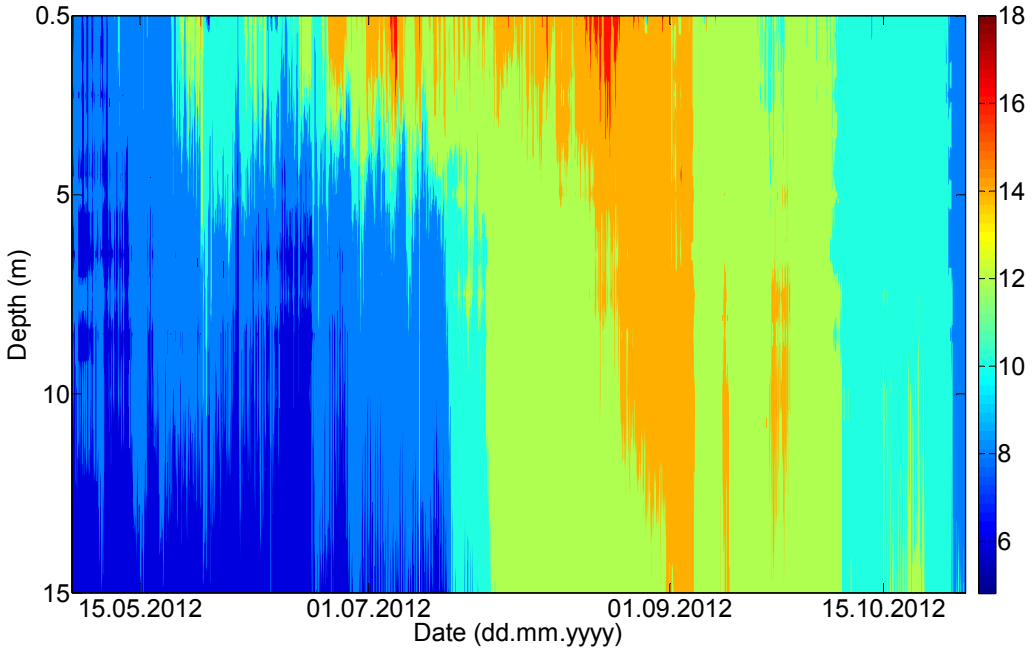

Figure 11: Temperatures logged during the sea-cage experiments at ACE. Vertical axis denotes depth in the water column, horizontal axis represents date and different colours denote different temperatures as provided by the colour bar on the right hand side.

.

Simulation experiments

To simulate the full-scale cases, the mathematical model was set up using cages of the same size as those used in the experiments (circumference 120 m, depth 12 m). These cages were stocked with simulated fish populations using the same mean weights as registered during cage stocking in the experiments. The fish were subjected to an environment featuring the feeding regime registered during the experiments, and temperature values (i.e. Figure 11) and light conditions similar to those measured in the experimental period. Full simulation of 120.000 individual fish over a period of 5-6 months with a time-step of 1 second would lead to extensive computation times, and would thus make the simulations unfeasible within a reasonable time frame. Consequently, the simulated population was set to 1.000 fish per cage rather than 120.000. To prevent the fish from being overfed in the simulations compared with in the experiments, the amount of feed delivered to each cage during feeding periods was reduced to about 1% of the original amount. This ensured that the amount of feed per kg fish was kept similar in simulations and experiments.

Simulation output in the form of individual dry weights were converted to wet weight values, and averaged for comparison with experimental data. Figure 12 through Figure 14 display the comparison between model output and experimental results.

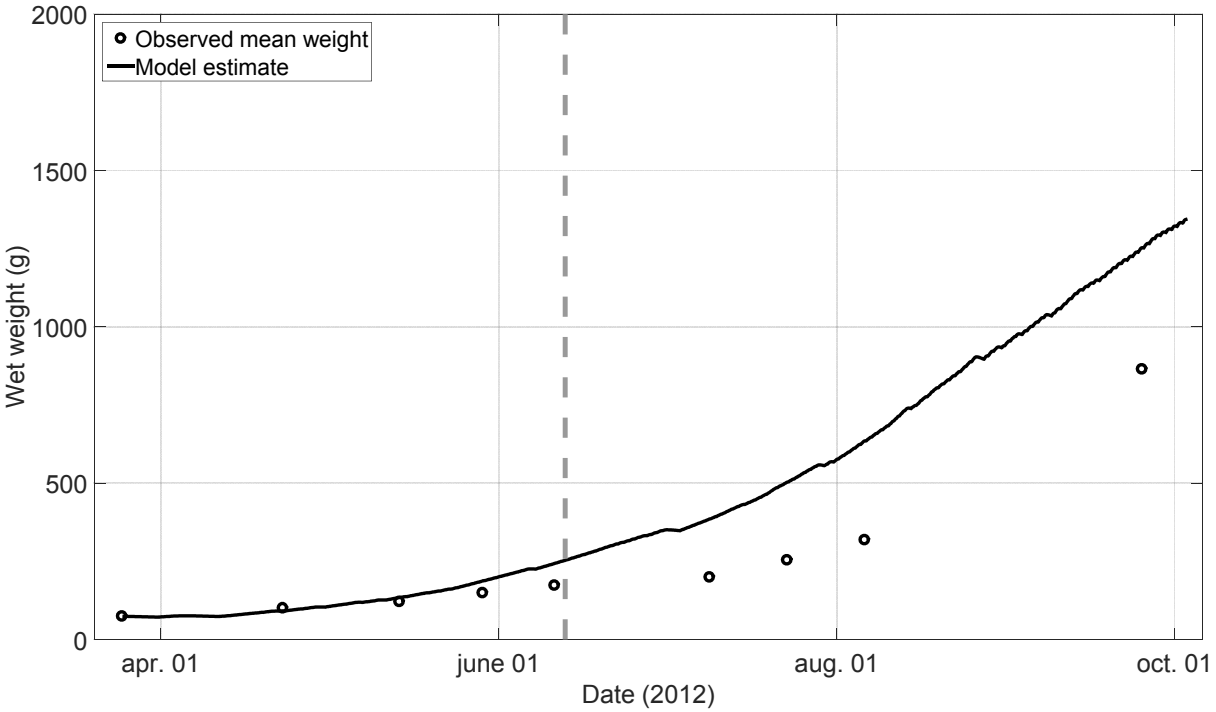

Figure 12: Comparison between observed mean weight in cage 5 (circles) and the corresponding model estimate (solid line). The vertical grey dashed line denotes the time at which PD was found in the cage.

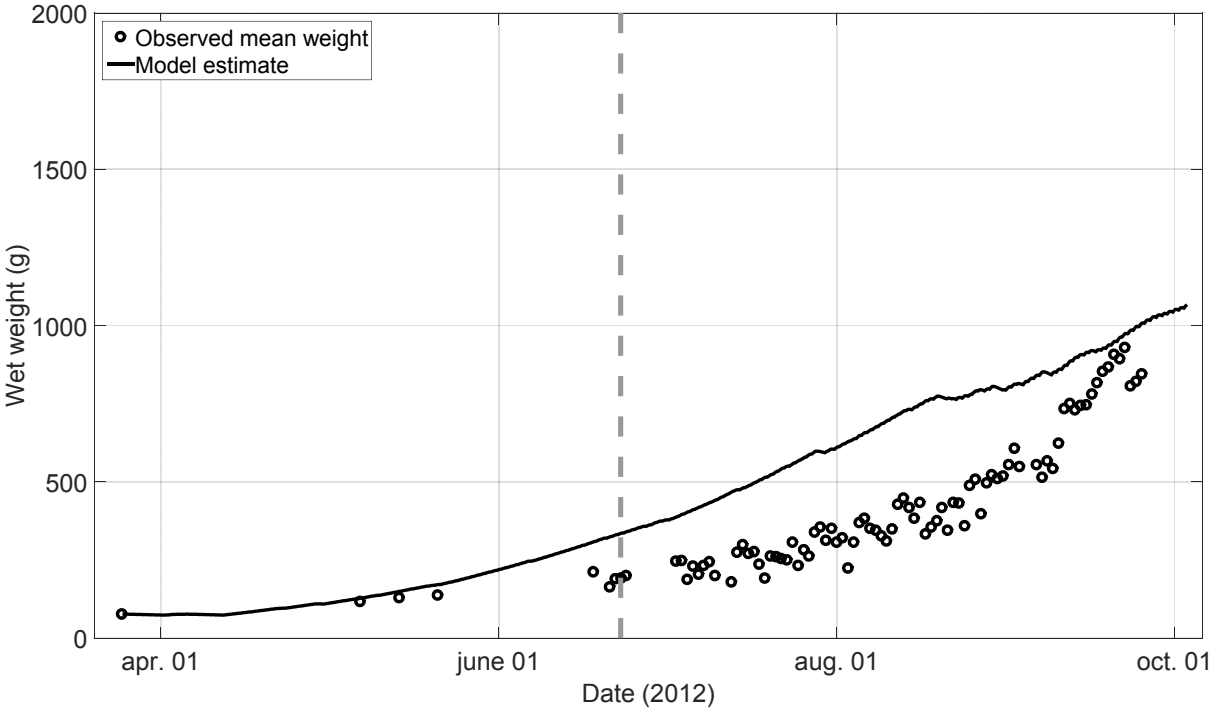

Figure 13: Comparison between observed mean weight in cage 6 (circles) and the corresponding model estimate (solid line). The vertical grey dashed line denotes the time at which PD was found in the cage.

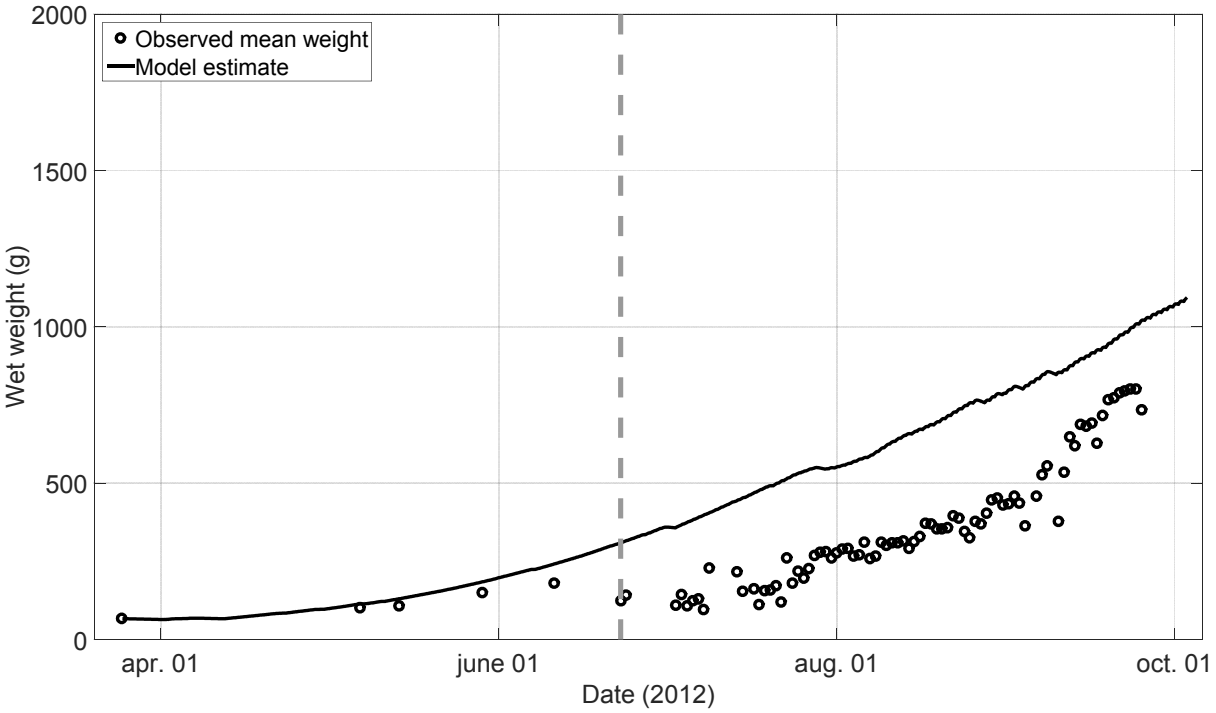

Figure 14: Comparison between observed mean weight in cage 7 (circles) and the corresponding model estimate (solid line). The vertical grey dashed line denotes the time at which PD was found in the cage.

Although the model predictions were close to the observed values prior to the disease outbreak, simulated growth rate in this period was somewhat higher than the growth rates observed in the experiments. This is also evident from the SGR-values in the period, which were higher than the observed values (Table 1).

Table 1: Observed and estimated SGR values for all three cages in the first half of the experimental period.

Cage number	Model estimate of SGR (%)	Experimental SGR (%)
5	1.5193	1.0806
6	1.6252	1.1862
7	1.6529	1.2782

Through the second half of the experiment, the model over-predicted the mean weight in all three cages. However, the growth rates as predicted by the model were similar to the growth rate in the observations, as seen by comparing the incline of the model estimate and the general trend in the observation data in all three cases. This is also seen in the SGR values for this interval (Table 2), which were very close to the observed values for cages 5 and 7, and simulated values for cage 6 slightly lower than the observed SGR. Deviations in SGR between simulated and observed values were generally lower for this period than for the first half of the experiment.

Table 2: Observed and estimated SGR values for all three cages in the second half of the experimental period.

Cage number	Model estimate of SGR (%)	Experimental SGR (%)
5	1.5005	1.5129
6	1.1604	1.3967
7	1.3213	1.3234

In cages 6 and 7 (Figure 13 and Figure 14), the observed growth increased towards the end of the experimental period, leading to higher growth rates than predicted by the simulation

model. This reduced the deviations between estimated and observed mean weights in these cages considerably, leading to that estimated and observed end weights were close. This effect was not observed in cage 5 (Figure 12), a feature which is also seen in that estimated SGR values for the entire period were more similar to observed SGR for cages 6 and 7 than for cage 5 (Table 3). Nonetheless, deviations between model estimate and experimental SGRs were low, despite the differences observed for the two periods separately.

Table 3: Observed and estimated SGR values for all three cages in the entire experimental period.

Cage number	Model estimate of SGR (%)	Experimental SGR (%)
5	1.5082	1.3297
6	1.3661	1.2995
7	1.4559	1.3042

3.2. Comparison with tank experiments

Setup of physical experiment

The tank experiments were conducted in a set of tanks ranging from 1 to 11 m in diameter, with the intent of identifying any scale dependent differences in fish performance when salmon are reared in indoor tanks and are provided with otherwise identical environmental conditions. In addition to different scales, the experimental period was divided into three distinct phases, the transport of 13.000 smolts from the hatchery being the first phase (Figure 15). During the second phase, the fish were divided into three groups, one of which was transferred directly to a set of 2 m tanks. The second group was placed in 1 m tanks while the third group was stocked in an 11 m tank. In the third phase, the fish in the 1 m tanks were transferred to 2 m tanks, while the fish in the 11 m tank were distributed between sets of 1 m, 2 m and 7 m tanks. This enabled an evaluation of whether the scaling history of the fish will impact fish performance.

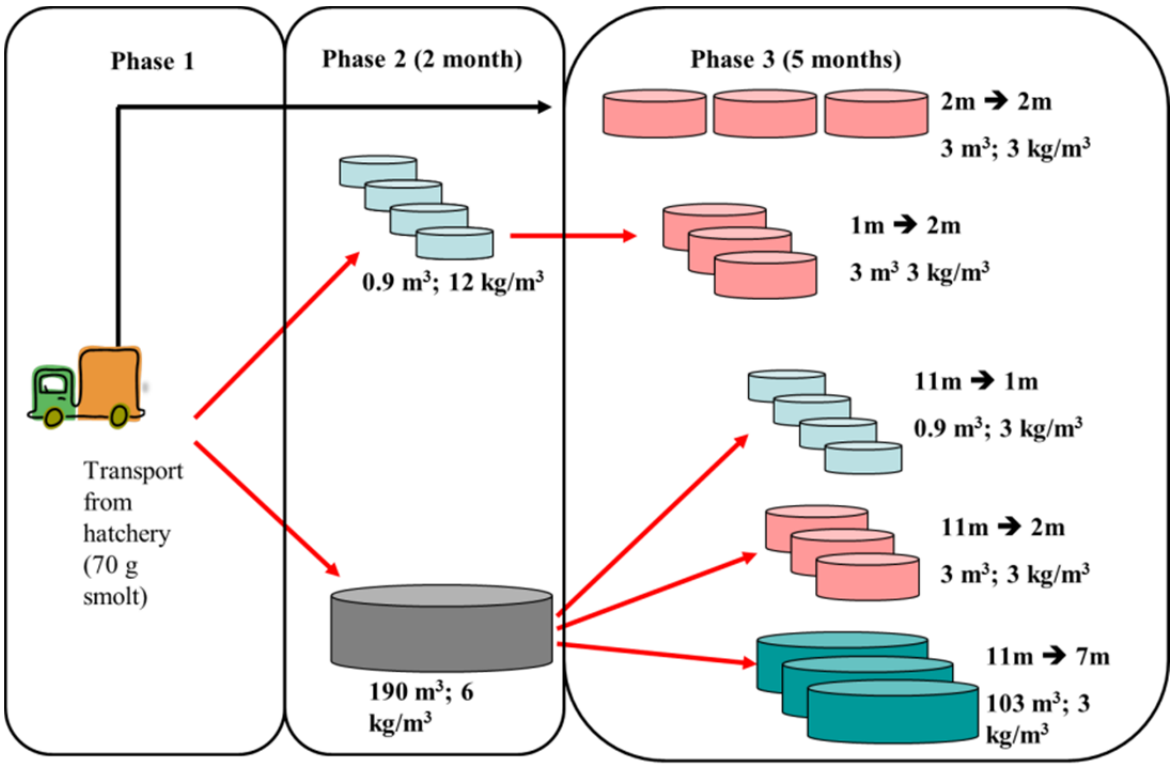

Figure 15: Outline of tank experiments illustrating the different physical scales and experimental phases (Figure from Deliverable 8.2).

All tanks used flow-through sea water rather than recirculation systems. Phase 3 was intended to be comparable to the full-scale sea-cage experiments. Production conditions in the tanks were therefore actively modified to match the conditions registered in the sea-cages as accurately as possible during this phase. This included temperature control on the inlet water to match the temperatures at 5 m in the sea-cages, and the application of a matching feeding regime both in terms of amount per kg fish and time of day. Furthermore, the lighting of the tanks was adjusted to the contemporary natural light period.

Weight and mortality levels were registered at the end of the experimental period. In addition, mean weight was estimated at the start of all three phases and at one point during phase 3 in July.

Experimental results

Results from the tank experiments revealed that growth performance and mortality depended on both the physical scale of the production units and the scaling history of the fish (Figure 16).

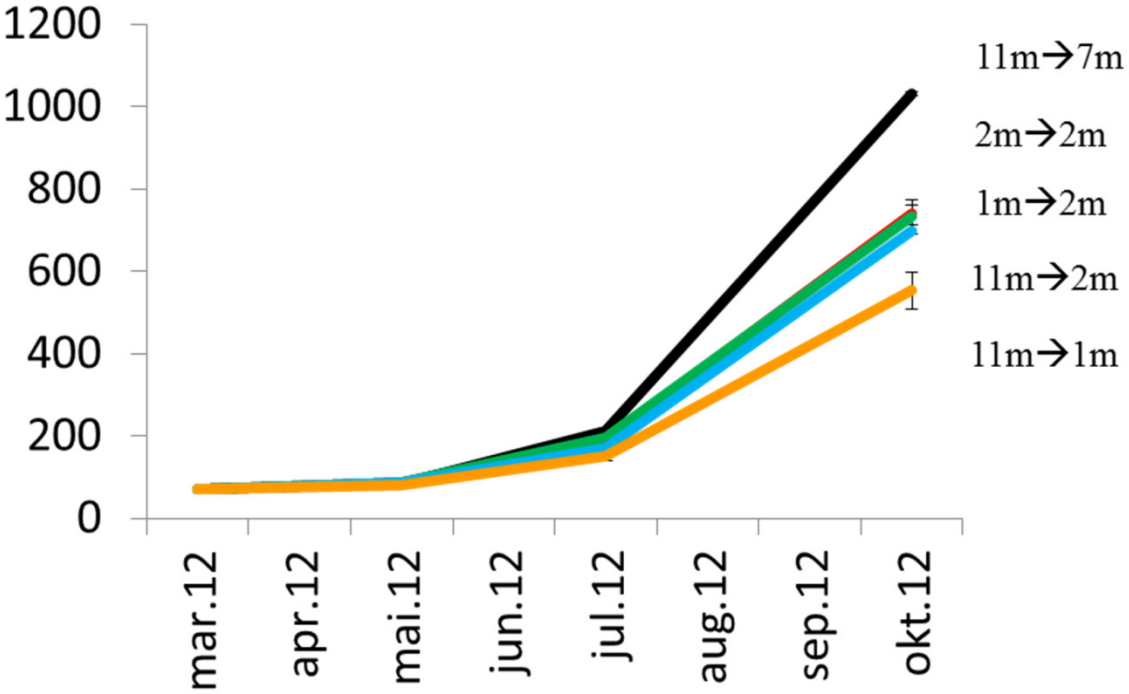

Figure 16: Growth results from tank experiments conducted at Nofima, Sunndalsøra. Different colours denote different treatments in phase 3 of the experiments, with black being the fish raised in 7 m tanks, red, green and blue being the fish raised in 2 m tanks, and orange being the fish raised in 1 m tanks.

The temperature control applied to the inlet water to the tanks ensured that temperatures were kept similar in all tanks, with the measurements obtained at 5 m depth at ACE as a reference. Light was supplied to the tanks through artificial lighting set up to follow the natural photoperiod throughout the experimental period.

See Deliverable 8.2 for more details and discussion of these results.

Simulation experiments

An important feature of the pellet distribution model is that it needs to retain full mass

balance in the transport of pellets between the cells used to discretise the production unit volume. Consequently, the feed model needs to be driven with a sufficiently short time step to ensure that pellet movements per time step are significantly shorter than the cell dimensions. At the same time, the discretisation of the volume needs to maintain sufficient resolution to produce a realistic spatial distribution of the feed. The smallest tank size used in the experiment (1 m diameter) was found to require very small cell sizes to obtain a sufficiently fine resolution, thus causing challenges in ensuring mass balance in the feed model and numerical issues. Consequently, the comparison between the numerical model and the experimental results was limited to encompass the 7 m and 2 m tanks in phase 3. To ensure some degree of comparability between the tanks and the full-scale trials, the 2 m tanks selected for simulation were the CompACE tanks which contained fish that were transferred directly to the 2 m tanks after arrival at Sunndalsøra.

The model was set up using parameters derived from the experimental setup, using cylindrical tanks with a radius of 3.5 m and a depth of 2.68 m for the 7 m tank, and radius and depth of 1 and 0.96 m respectively for the 2 m tank. Feed input data from the experiments was used as a direct input to set up the feeding model, whereas the temperatures measured in the tanks throughout the experiment was used as an input-dataset on temperature. The fish populations were initialised using the mean ± standard deviation in weight. For the 2 m tanks, the population size used in the simulations (114) matched the number of individual fish registered at the start of phase 3. The 7 m tank was set up with a smaller number of individuals (750) than in the experiments (3864) to prevent extensive computation times for the simulation scenario. Figure 17 and Figure 18 display the comparison between model output and observational data for the 2 m and 7 m tanks respectively.

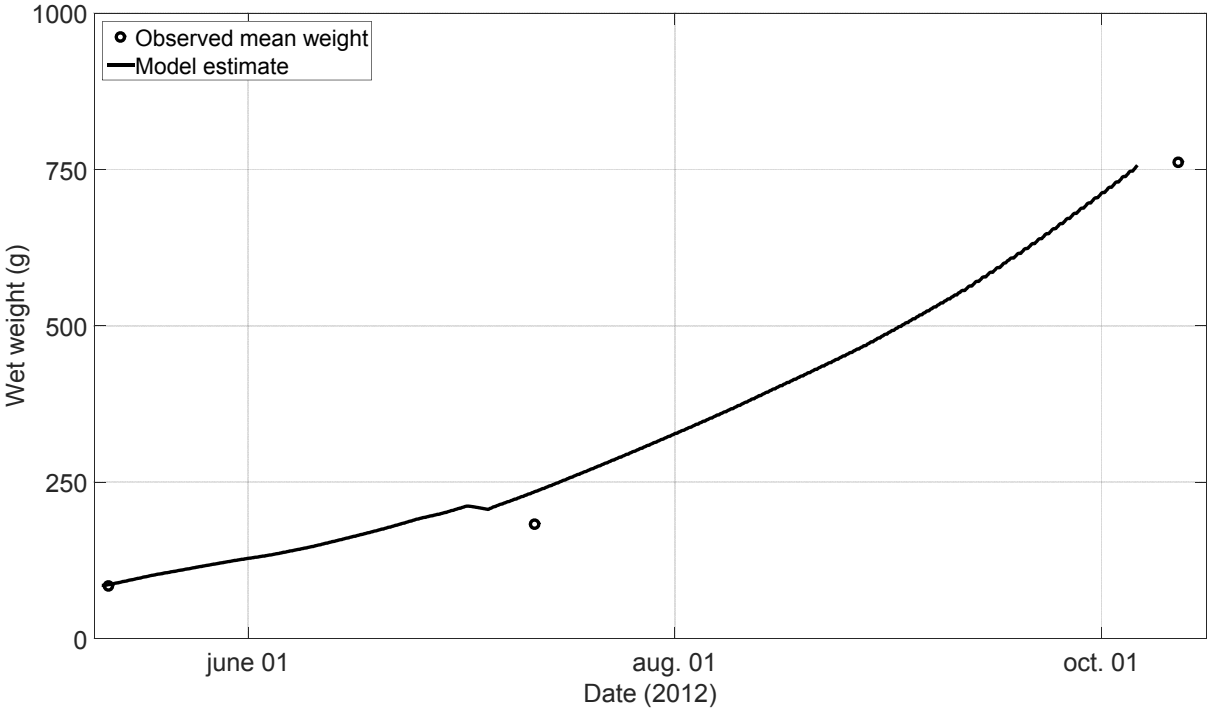

Figure 17: Comparison between observed mean weight in 2 m diameter tank number 201 (circles) and the corresponding model estimate (solid line).

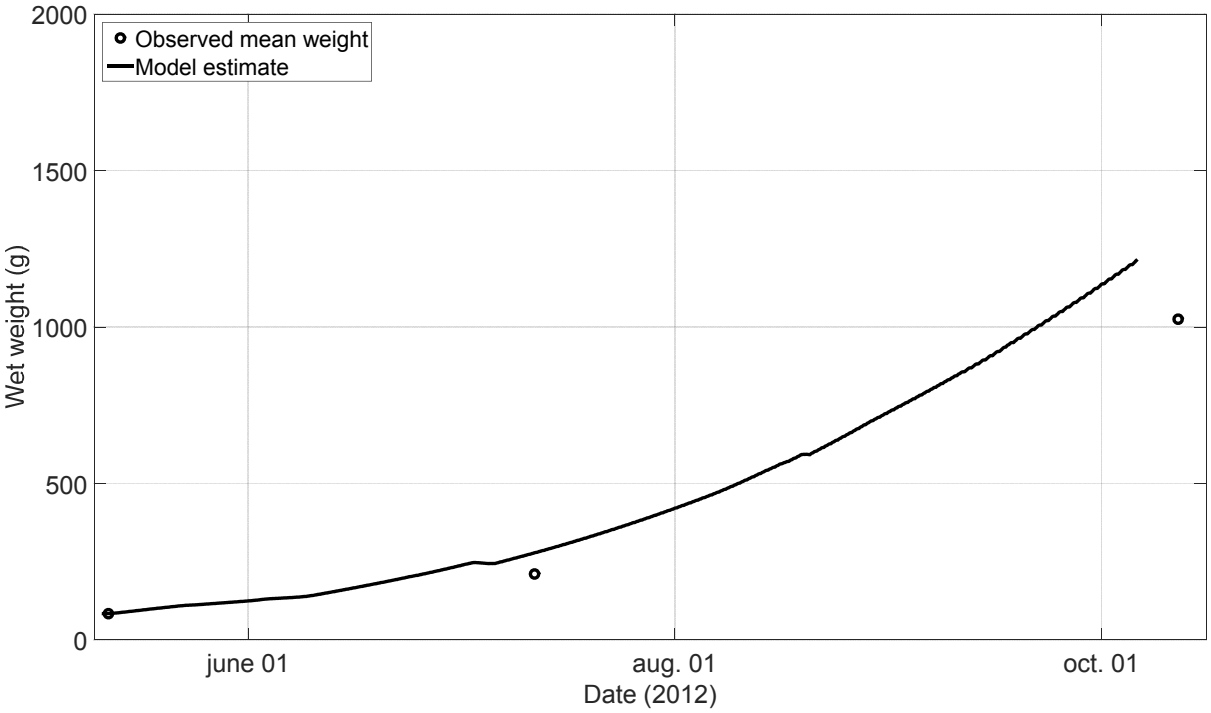

Figure 18: Comparison between observed mean weight in 7 m diameter tank number 4 (circles) and the corresponding model estimate (solid line).

Although the growth trajectory predicted by the model was close to the intermediate value in the observational dataset for the 2 m tank (Figure 17), the model seemed to overestimate the growth of the fish in the first few months of the experiment. This is also seen in that the estimated SGR for this period is higher than the observed value (Table 4). For the 7 m tank (Figure 18), the model predicted higher growth rates than in the 2 m tank. Similarly to for the 2 m tank, the model overestimated the growth in the first period for the 7 m tank (Table 4).

Table 4: Observed and estimated SGR values for the 2m and 7m tanks used in the simulations between start and intermediate weight measurement.

Tank number (diameter)	Model estimate of SGR (%)	Experimental SGR (%)
4 (7m)	1.9374	1.512
201 (2m)	1.6429	1.2684

Despite there being no data points between the intermediate and the final value in the observation data for the tanks, the model seemed to slightly underestimate the growth of the fish for this period. This is also apparent in simulated vs. observed SGR values (Table 5). For the 7 m tank, the simulated relative growth rate was approximately the same as in the observations, as can be seen from the SGR values (Table 5).

Table 5: Observed and estimated SGR values for the 2m and 7m tanks used in the simulations between intermediate weight measurement and experiment end.

Tank number (diameter)	Model estimate of SGR (%)	Experimental SGR (%)
4 (7m)	1.7099	1.7169
201 (2m)	1.3571	1.5474

The final value of the simulation came close to the end value in the observational data for the 2 m tank. This is also seen in that the estimated and observed SGR values for the entire period were almost identical (Table 6). For the 7 m tank, the model's overestimate of growth in the first period was retained through the experimental period, giving a higher overall growth rate compared with the observations (Table 6).

Table 6: Observed and estimated SGR values for the 2m and 7m tanks used in the simulations for the entire experimental period.

Tank number (diameter)	Model estimate of SGR (%)	Experimental SGR (%)
4 (7m)	1.8051	1.6352
201 (2m)	1.4767	1.4362

4. Discussion and conclusion

4.1. Model verification and validation

In all simulation cases, the model predicted a higher growth at the beginning of the experimental period than was registered in the experiments. A possible reason behind this is that the fish, after having recently been handled and transferred, were displaying a mild stress response. Such an effect could cause a time lag in growth where the fish would need some time in order to get adjusted to their novel surroundings and thus also be able to ingest and assimilate feed at a normal rate. This factor has not been included in the model, as there is little information about the post-transfer effects of salmon in literature. In the simulation model, the fish were therefore predicted to feed at a normal rate, allowing them to start growing at an earlier point in time. There was also increased mortality in the initial phase after transfer to the experimental tanks, and in the period affected by PD in the sea cages, and this can have a side effect on the growth rate at the population level if smaller or larger fish is overrepresented in the mortality.

An additional factor that might have contributed to higher growth rates early in the period is that the water temperature could have a stronger regulatory effect on fish appetite than assumed in the energetic model. At present, the only effect temperature has on fish appetite in the model is that it controls the stomach evacuation rate of the fish. This is a well-founded assumption, but it is possible that it is either too weak in the present model, or that temperature impacts appetite in additional manners. Water temperature increased throughout the experimental period, thus a stronger link between temperature and appetite could be tuned to provide lower growth rates for the first half of the experimental periods, and likewise higher growth in the remainder of the trial. Such a change would probably allow for a better fit between model estimates and experimental data in all cases included in this deliverable.

To reduce the computational load of the simulations, the simulation results presented for the 7 m tank and the cages were acquired using a smaller population than used in the experiments. The reduction of feed amounts delivered to the cages/tanks in the simulations was intended to remedy eventual consequences this would have for feed intake as the amount of feed per individual fish was then kept equal to that applied in the experiments. Reducing the population size could also influence feeding responses in that the each individual fish would then have more space for movement and be less affected by the presence of their conspecifics. A series of short simulation experiments where the number of individuals were varied were conducted to test this effect. The results from these simulations indicated that average feed intake of the fish in the cages/7 m tanks stabilised when using around 500 individual fish, indicating that the scaling of feed amounts was sufficient to account for most of the effects population size will have on the feed intake of the fish. Furthermore, this is in accordance with feeding management practices in the industry which are designed to ensure that all the fish are offered sufficient feed to maintain acceptable growth rates, meaning that the feeding schedule should be adapted to population size.

Another aspect of using a smaller population size could be that individual fish in a less densely populated cage could more easily assume positions in the cage where abiotic

conditions (e.g. temperature, light) are within preferable ranges, possibly leading to better growth conditions. However, in these experiments, the fish density was less than 9 fish per m^3 (or less than 1 kg fish per m^3 initially), meaning that the abilities of a simulated individual in assuming positions with beneficial conditions was probably not strongly affected by fish density. Furthermore, temperatures at ACE were found to vary little through the water column for extended segments of the experimental period (Figure 11) suggesting that thermal conditions were similar in most of the cage volume. Since the temperatures in the tanks were regulated through thermal adjustment of the influx water, there was probably low spatial variability in temperature throughout the tank volumes. Hence, fish density was unlikely to have had a major impact on growth through spatially inhibiting individuals from experiencing the most beneficial conditions.

Although simulations using the full populations from the experiments were not possible to conduct in time for this deliverable, such simulations will be done in the future to ensure that scaling effects of population size are fully accounted for.

Comparisons with full-scale experiments

Since model predictions were close to the observed values in the period preceding the outbreak of PD for all three cages, it is likely that the model features the major mechanisms for growth of healthy Atlantic salmon in a full-scale culture setting. Data on feed and temperature were directly adapted from the experimental results, thus the simulated fish were exposed to the same external influences as the fish in the physical experiment. The good correspondence thus further implies that the model was able to realistically predict the feed intake of the individual fish for this period, which represents the primary influence on fish growth in the model. Feed intake for each individual is computed each time step (i.e. each second) in the model, thus even small errors in this feature could cause large deviations which cumulatively increase with simulation time. Considering the long duration of the pre-disease period, it is thus likely that the model representation of feed intake captures the main dynamics behind feed intake in healthy farmed Atlantic salmon.

The lack of a representation of the inhibiting effects of PD on fish growth is likely one of the main explanations behind the larger deviations between model output and experimental data observed after the disease outbreak. It has not been an aim of the present model to represent salmon under the influence of disease. Such effects have been identified in several clinical studies (McLoughlin et al., 2002, McLoughlin and Graham, 2007), but are generally difficult to describe quantitatively. This renders these effects difficult to include in a mathematical model, as quantitative measures are required to derive mathematical functions estimating such dynamics.

Environmental conditions were within ranges that should not have adverse effects on fish growth throughout the experimental period, thus the growth as estimated by the model was closely linked with the feed input to the cages. This is seen by comparing the trajectories for individual mean weight as estimated by the model and with the cumulative feed delivery for cages 5, 6 and 7 (Figure 19 through Figure 21).

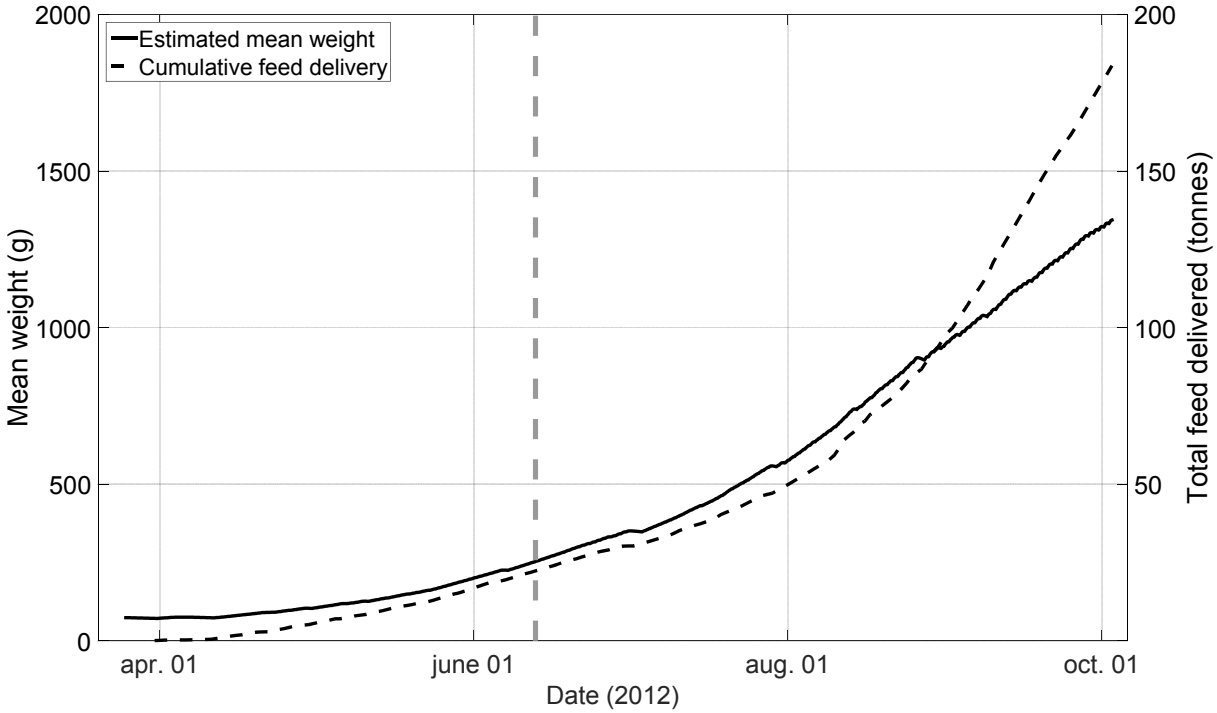

Figure 19: Estimated average individual fish wet weight in cage 5 (solid line) and cumulative feed delivery to cage 5 (dashed black line) over the experimental period. Vertical grey dashed line represents the time at which PD arose in the cage. Horizontal axis represents date, while vertical axes represent mean weight in g (left) and total cumulative feed delivered to the cage in tonnes (right).

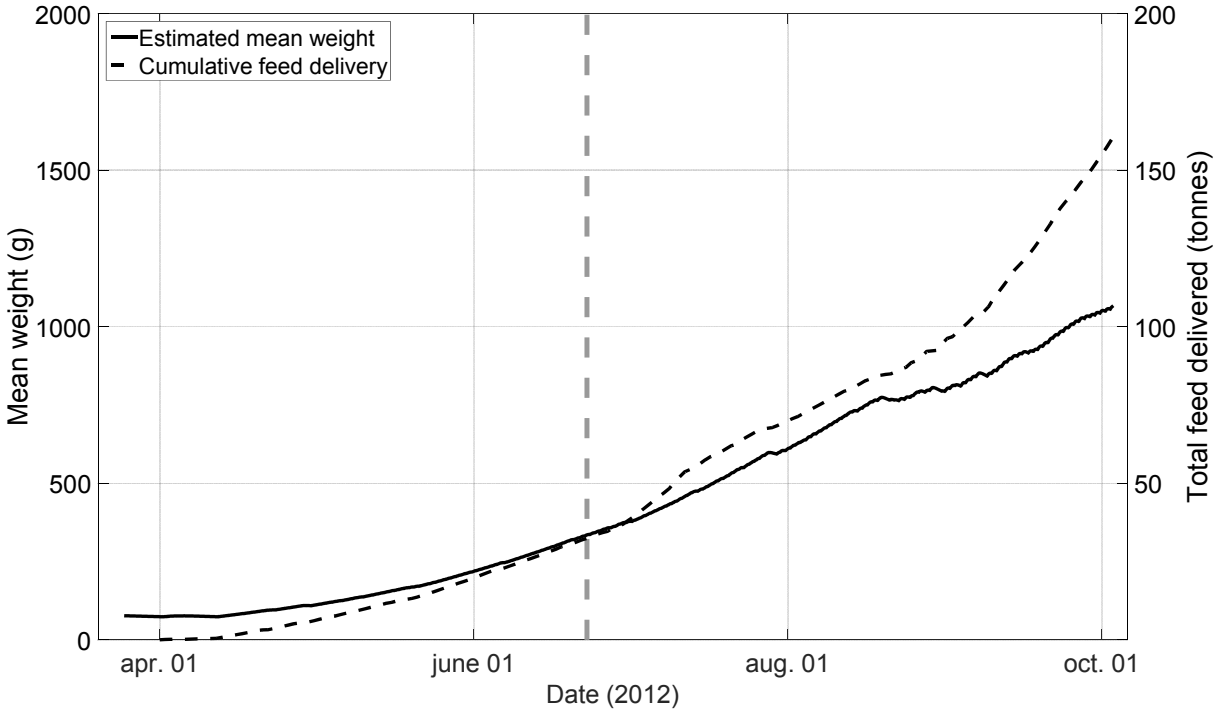

Figure 20: Estimated average individual fish wet weight in cage 6 (solid line) and cumulative feed delivery to cage 6 (dashed black line) over the experimental period. Vertical grey dashed line represents the time at which PD arose in the cage. Horizontal axis represents date, while vertical axes represent mean weight in g (left) and total cumulative feed delivered to the cage in tonnes (right).

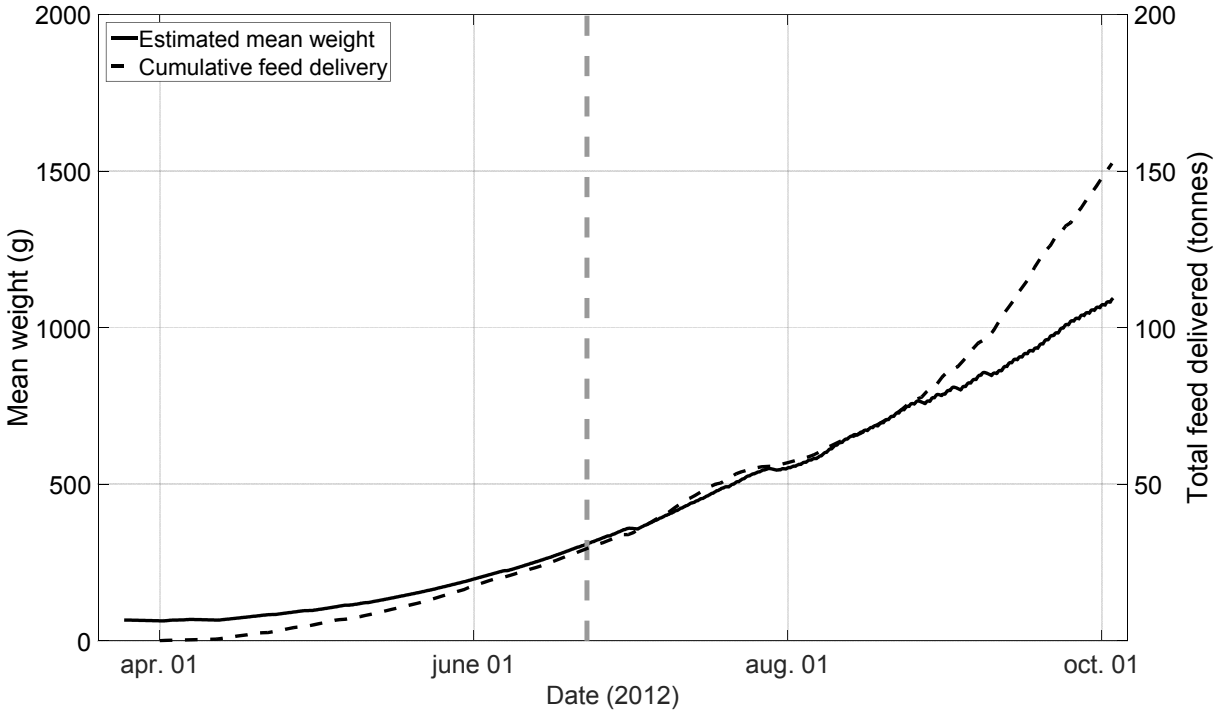

Figure 21: Estimated average individual fish wet weight in cage 7 (solid line) and cumulative feed delivery to cage 7 (dashed black line) over the experimental period. Vertical grey dashed line represents the time at which PD arose in the cage. Horizontal axis represents date, while vertical axes represent mean weight in g (left) and total cumulative feed delivered to the cage in tonnes (right).

In addition to affecting the mortality and growth of salmon, PD is known to reduce the appetite of infected fish (McLoughlin et al., 2002). To countermand the potentially excessive feed losses this situation could induce, farmers typically reduce the feeding rate once disease has been found in the fish farm. When the fish appear to have escaped the most virulent disease period, the feeding rates are then readjusted to higher levels, possibly with even higher rates than prior to the disease outbreak to stimulate compensatory growth. This particular method of reducing feed loss appeared to have been applied to the cages in the full-scale experiments in task 8.2, exemplified by the cumulative feed delivery to all three cages. The inclines of the curves displaying feed were lower between the time of the disease outbreak (July) and September, after which the incline was higher, indicating higher feed delivery rates. In cages 6 (Figure 13) and 7 (Figure 14), the experimental fish exhibited higher growth rates than the rates estimated by the model after September. This coincided with the period in which the incline of cumulative feed delivery was highest in both cages (Figure 20 and Figure 21), suggesting that this was indeed compensatory growth stimulated by an increased access to feed. Since the model did not include any representation of PD, the mechanisms inducing compensatory growth in fish after disease were also not modelled, probably explaining why the increase in growth rate seen in the experimental data did not occur in the model output.

For all three cages, the estimated growth trajectory followed trend in cumulative feed delivery until about 1 month of the period remained (Figure 19 through Figure 21). After this point, the growth rate (indicated by the incline of the weight estimate curve) was clearly lower than the increases in supply of feed (indicated by the incline of the cumulative feed curve). A likely explanation for this is that the increased maintenance costs of the estimated fish at this point exceeded the gradual increase in feed delivery, thus leaving less energy for structural growth. The match between model output and observational data was lowest for cage 5. Albeit the data from this cage contained fewer data points than the datasets from the other cages, and thus should be seen as a less definite result, the reason behind these deviations

may be that this particular cage was more strongly afflicted by PD than the other cages (ACE, pers. comm.). This observation is strengthened by cage 5 receiving in total 15-20% more feed than the other cages (Figure 19). In not having a reduction in appetite due to PD, the model thus simulated the response of a healthy fish population toward the delivered amount, leading to a higher discrepancy between observations and model results.

Comparisons with tank experiments

The model was able to predict the growth in the 2 m tank, indicating that the model captured the main dynamics of salmon growth in small indoor tanks. The main impact factors behind fish growth (feed supply and temperature) were directly adapted from the setup used in the experiments, thus exposing the simulated fish to the same conditions as the fish in the experiments. Similarly to the full-scale experiments, this suggests that the feeding model produced realistic intake rates on an individual level. For the 7 m tank, the model showed a similar relationship to the observations, with an overestimation of growth rate up to the intermediate measurement and better match with observed growth rate after the intermediate measurement. Overall, the model overestimates the growth to a greater degree in the 7 m tank than in the 2 m tank, meaning that the higher growth rates observed in the 7 m tank were reproduced by the model.

In both tanks, the model gives higher than observed growth in the first part of the experimental period. This deviation may be caused by an acclimatisation period after the transfer of the fish to the experimental tanks. Both 7 m and 2 m tanks showed elevated mortality initially after transfer of the fish (see D8.2). It would be reasonable for the fish to display lower feed ingestion rates and lower growth in this period, but growth was not measured until two months after the transfer. The model includes no such effects, potentially leading it to overestimate initial growth rates. Adding an initial lag phase to the tank simulations would give a significantly better fit at the time of the intermediate measurements, and the growth rates in the second part of the period already show fairly good agreement.

4.2. Scale effects in model simulations

Since it was not feasible to conduct reliable simulations of the smallest tank size (1 m), the only comparison with regard to scale possible was between the 7 m tank and the 2 m tank. In the experiments, the fish in the 7 m tanks were found to display significantly higher growth rates than in either the 2 m or the 1 m tanks (Deliverable 8.2). This effect was reproduced in the simulation data in that the model reproduced both growth trajectories with relatively high precision, implying that the model reflected the differences in fish performance between the tanks of different physical scales. Furthermore, although the results from the indoor tanks may not be directly comparable with the results from sea-cages, the model predicted the major features and end weights in the growth trajectories registered in the cages. Since the model was run with an identical set of behavioural and energetic parameters for cages and tanks, this suggests that the model was also able to estimate most differences in growth dynamics between full-scale cages and indoor tanks.

The model does not include all factors identified as possible scale factors in aquaculture production of fish (see Deliverable 8.1, Appendix 3), as many of these were difficult to model based on the present literature. However, the results from the simulations presented here suggest that the model featured the primary drivers behind scale-dependent effects on fish performance. Of potential scale factors included in the model, temperature was unlikely to retain a role in producing the scale difference between tank sizes as temperatures were kept the same in 7 and 2 m tanks throughout the experiments, a similarity that was included in the model simulations. Between the tanks and the cages, however, temperature could contribute to differences in fish performance, as the caged fish were able to regulate their swimming depth in response to temperature differences whereas the tank raised fish were subjected to

a single water temperature irrespective of location within the unit. Although there was little vertical variability in temperature in the ACE cages at times throughout the experimental period, there were some variations, especially early in the experiment (Figure 11) that could influence fish growth.

The geometric size of the production unit itself represents another factor in the model that could be contributing to the scale dependent differences in fish performance. While the physical scale of the production unit is unlikely to have a direct effect on the growth of the fish, it may have indirect effects by affecting the retention time of the feed in the production volume. Smaller (and especially shallower) production units will give the fish less time to capture the feed before it reaches the tank bottom (or walls in case of a net-cage) upon which it is assumed to be removed from the system. This will influence the chance that a pellet is detected, captured and ingested before it exits the system, thus impacting the feed intake of the fish which again is closely linked with the growth performance of the fish. Furthermore, the feed intake of the fish is affected by how well the pellets are dispersed in the water volume. The distribution pattern of the feed will vary with physical scale, and may potentially have a large effect on how available the feed is for the fish. Physical size will set the finite limits for how dispersed the feed may become, and also plays a crucial role in the formation of the flow patterns within the unit. Flow patterns will typically be a key factor in determining the distribution of feed as it represents the main component in pellet advection between cells in the grid structure.

In essence, these results indicate that the model at present is able to capture scaling effects on fish performance in aquaculture production units. However, we cannot fully conclude at this point since the scale effects in the experiments may have led to differences in feed input, which may have contributed toward imposing the scale effects seen in the model. The present simulations verify that the model to a satisfactory degree reproduces the dynamics of the experiments, but to investigate scale effects in the model a new set of simulations must be run.

4.3. Conclusions, further work and application areas

The main aim behind the model presented here was to provide a virtual tool for predicting eventual differences in fish performance between production units of different physical scales. In this regard, the model was shown to have a good potential in that it indicated differences in performance between tanks of two different scales (2 and 7 m circumference), and between tanks and full-scale industrial sea-cages. The model must now be used in further simulations providing equal conditions in terms of environment, density of fish and feed delivery relative to the biomass, over different scales in order to specifically test for scale effects. There are a number of potential scale effects that may be present, some of which are not currently included in the model. By including these separately or in combinations the model can be used to test such hypotheses in a systematic fashion.

At present, the model does not include activity levels as a factor in the calculated maintenance costs of growth. Some behavioural traits, such as increased swimming speeds, are likely to increase the energetic costs of the fish, thus having an impact on the energy budget of the animal. There is little available knowledge on the actual magnitude of such energetic costs, but it may be possible to derive a mathematical expression for this based on the assumed oxygen consumption of salmon when swimming at different speeds. Such an expansion would improve the model in that it could take into account the effects on fish performance caused by scale-induced current differences. This may be especially interesting when considering tanks, as salmon produced in tanks tend to be exposed to more constant flow fields than fish reared in cages (in which currents will fluctuate with tides and other externally induced drivers). It is reasonable to assume that fish reared in tanks with larger

diameters and thus higher current speeds near the edges, would expend more energy on maintaining position than fish reared in smaller tanks.

One future task that remains with this model is to conduct a more exhaustive simulation study of the different tanks used in the on-land experiments presented in Deliverable 8.2. Although the present document only includes the results from one tank of 2 and one tank of 7 m diameter, the experimental study featured several tanks of 1, 2 and 7 m diameter. Each tank for each physical scale were offered similar abiotic conditions and exposed to roughly the same feeding regime. However, a simulation of all the different tanks for each scale could produce a better foundation for the conclusions drawn at present. Such a study is expected to show the same correspondence between model output and observation data for all cases at each physical scale.

Beyond its role as a tool for investigating scale effects, this model system represents an attempt at a holistic model system describing the dynamics of a rearing unit for Atlantic salmon. It is easy to see a number of alternative uses for the model, for instance as a tool for studying feeding strategies and minimization of feed loss, or for investigating the effect of environmental parameters and management strategies to optimize production.

The experimental work in WP8 also covered scaling effects in larval and juvenile sea bass (see D8.2). This model can be applied to juvenile sea bass by conducting fairly moderate changes to the model, primarily by changing the DEB model parameters and by modifying the behaviour sub-model so that it reflects the behaviour of sea bass.

References

AKSNES, A., GJERDE, B. & ROALD, S. O. 1986. Biological, chemical and organoleptic changes during maturation of farmed Atlantic salmon, Salmo salar. *Aquaculture,* 53**,** 7-20.

ALVER, M., ALFREDSEN, J. & OLSEN, Y. 2006. An Individual-based Population Model for Rotifer (<i>Brachionus plicatilis</i>) Cultures. *Hydrobiologia,* 560**,** 93-108.

ALVER, M. O., ALFREDSEN, J. A. & SIGHOLT, T. 2004. Dynamic modelling of pellet distribution in Atlantic salmon (Salmo salar L.) cages. *Aquacultural Engineering,* 31**,** 51-72.

ALVER, M. O., ALFREDSEN, J. A. & ØIE, G. 2007. Estimating larval density in cod (*Gadus morhua*) first feeding tanks using measurements of feed density and larval growth rates. *Aquaculture,* 268**,** 216-226.

ALVER, M. O., FØRE, M., SKØIEN, K. R., AAS, T. S., OEHME, M. & ALFREDSEN, J. A. In preparation. Modelling and optimization of feed distribution in sea cages.

AUSTRENG, E., STOREBAKKEN, T. & ASGARD, T. 1987. Growth-Rate Estimates for Cultured Atlantic Salmon and Rainbow-Trout. *Aquaculture,* 60**,** 157-160.

BLEVINS, R. D. 2003. *Applied fluid dynamics handbook*, Krieger Publishing Company, Malabar, US.

DAVIDSON, J. & SUMMERFELT, S. 2004. Solids flushing, mixing, and water velocity profiles within large (10 and 150 m^3) circular 'Cornell-type' dual-drain tanks. *Aquacultural Engineering,* 32**,** 245-271.

DEMPSTER, T., JUELL, J.-E., FOSSEIDENGEN, J. E., FREDHEIM, A. & LADER, P. 2008. Behaviour and growth of Atlantic salmon (< i> Salmo salar</i> L.) subjected to short-term submergence in commercial scale sea-cages. *Aquaculture,* 276**,** 103-111.

FREDHEIM, A. 2005. *Current forces on net structures.* PhD, Norwegian University of Science and Technology.

FØRE, M., DEMPSTER, T., ALFREDSEN, J. A., JOHANSEN, V. & JOHANSSON, D. 2009. Modelling of Atlantic salmon (*Salmo salar* L.) behaviour in sea-cages: A Lagrangian approach. *Aquaculture,* 288**,** 196-204.

FØRE, M., DEMPSTER, T., ALFREDSEN, J. A. & OPPEDAL, F. 2013. Modelling of Atlantic

salmon (*Salmo salar* L.) behaviour in sea-cages: Using artificial light to control swimming depth. *Aquaculture,* 388**,** 137-146.
GANSEL, L. C., RACKEBRANDT, S., OPPEDAL, F. & MCCLIMANS, T. A. Flow fields inside stocked fish cages and the near environment. ASME 2011 30th International Conference on Ocean, Offshore and Arctic Engineering, 2011. American Society of Mechanical Engineers, 201-209.
HANDELAND, S. O., IMSLAND, A. K. & STEFANSSON, S. O. 2008. The effect of temperature and fish size on growth, feed intake, food conversion efficiency and stomach evacuation rate of Atlantic salmon post-smolts. *Aquaculture,* 283**,** 36-42.
HANDÅ, A., ALVER, M., EDVARDSEN, C. V., HALSTENSEN, S., OLSEN, A. J., ØIE, G., REITAN, K. I., OLSEN, Y. & REINERTSEN, H. 2011. Growth of farmed blue mussels (*Mytilus edulis* L.) in a Norwegian coastal area; comparison of food proxies by DEB modelling. *J. Sea Res.,* 66**,** 297-307.
HARLOW, F. H. 2004. Fluid dynamics in Group T-3 Los Alamos National Laboratory: (LA-UR-03-3852). *Journal of Computational Physics,* 195**,** 414-433.
KIRK, J. T. O. 1994. *Light and Photosynthesis in Aquatic Ecosystems*, Cambridge University Press.
KOOIJMAN, S. A. L. M. 2000. *Dynamic energy and mass budgets in biological systems*, Cambridge University Press.
KOSKELA, J., PIRHONEN, J. & JOBLING, M. 1997. Feed intake, growth rate and body composition of juvenile Baltic salmon exposed to different constant temperatures. *Aquaculture International,* 5**,** 351-360.
LADER, P., DEMPSTER, T., FREDHEIM, A. & JENSEN, O. 2008. Current induced net deformations in full-scale sea-cages for Atlantic salmon (Salmo salar). *Aquacultural Engineering,* 38**,** 52-65.
LØLAND, G. 1993. *Current forces on and flow through fish farms.* PhD, Norwegian University of Science and Technology.
MARAFIOTI, G., ALFREDSEN, J. A. & ALVER, M. O. Estimation of growth in farmed Atlantic salmon *Salmo salar* L. based on Dynamic Energy Budget (DEB) model and Kalman filtering. Poster at the European Aquaculture Society (EAS) Aquaculture Europe Conference, 2012 Prague, Czech Republic.
MCLOUGHLIN, M. & GRAHAM, D. 2007. Alphavirus infections in salmonids–a review. *Journal of fish diseases,* 30**,** 511-531.
MCLOUGHLIN, M., NELSON, R., MCCORMICK, J., ROWLEY, H. & BRYSON, D. 2002. Clinical and histopathological features of naturally occurring pancreas disease in farmed Atlantic salmon, Salmo salar L. *Journal of fish diseases,* 25**,** 33-43.
MCVICAR, A. 1987. Pancreas disease of farmed Atlantic salmon, *Salmo salar*, in Scotland: Epidemiology and early pathology. *Aquaculture,* 67**,** 71-78.
MONAGHAN, J. J. 1992. Smoothed particle hydrodynamics. *Annual review of astronomy and astrophysics,* 30**,** 543-574.
OEHME, M., AAS, T. S., SØRENSEN, M., LYGREN, I. & ÅSGÅRD, T. 2012. Feed pellet distribution in a sea cage using pneumatic feeding system with rotor spreader. *Aquacultural Engineering,* 51**,** 44-52.
OLSEN, O. A. & BALCHEN, J. G. 1992. Structured modeling of fish physiology. *Mathematical biosciences,* 112**,** 81-113.
PECQUERIE, L., PETITGAS, P. & KOOIJMAN, S. A. L. M. 2009. Modeling fish growth and reproduction in the context of the Dynamic Energy Budget theory to predict environmental impact on anchovy spawning duration. *Journal of Sea Research,* 62**,** 93-105.
PEETERS, F., LI, J., STRAILE, D., ROTHHAUPT, K. O. & VIJVERBERG, J. 2010. Influence of low and decreasing food levels on Daphnia-algal interactions: Numerical experiments with a new dynamic energy budget model. *Ecological Modelling,* 221**,** 2642-2655.
ROSLAND, R., STRAND, Ø., ALUNNO-BRUSCIA, M., BACHER, C. & STROHMEIER, T. 2009. Applying Dynamic Energy Budget (DEB) theory to simulate growth and bio-

energetics of blue mussels under low seston conditions. *Journal of Sea Research,* 62**,** 49-61.

TALBOT, C., CORNEILLIE, S. & KORSØEN, Ø. 1999. Pattern of feed intake in four species of fish under commercial farming conditions: implications for feeding management. *Aquaculture Research,* 30**,** 509-518.

VAN DER MEER, J. 2006. An introduction to Dynamic Energy Budget (DEB) models with special emphasis on parameter estimation. *Journal of Sea Research,* 56**,** 85-102.

VAN DER VEER, H. W., CARDOSO, J. F. M. F. & VAN DER MEER, J. 2006. The estimation of DEB parameters for various Northeast Atlantic bivalve species. *Journal of Sea Research,* 56**,** 107-124.

Annex 1

Deliverable Check list (to be completed by Deliverable leader)

	Check list		Comments
BEFORE	I have checked the due date and have planned completion in due time	X	*Please inform Management Team of any foreseen delays*
	The title corresponds to the title in the DOW	X	*If not please inform the Management Team with justification*
	The dissemination level corresponds to that indicated in the DOW	X	
	The contributors (authors) correspond to those indicated in the DOW	X	
	The Table of Contents has been validated with the Activity Leader	X	*Please validate the Table of Content with your Activity Leader before drafting the deliverable*
	I am using the AQUAEXCEL deliverable template (title page, styles etc)	X	*Available in "Useful Documents" on the collaborative workspace*
The draft is ready			
AFTER	I have written a good summary at the beginning of the Deliverable	X	*A 1-2 pages maximum summary is mandatory (not formal but really informative on the content of the Deliverable)*
	The deliverable has been reviewed by all contributors (authors)	X	*Make sure all contributors have reviewed and approved the final version of the deliverable. You should leave sufficient time for this validation.*
	I have done a spell check and had the English verified	X	*Ask a colleague with a good level of English to review the language of the text and do a spell-check too.*
	I have sent the final version to the Activity Leader and to the 2nd Reviewer for approval	X	*Send the final draft to your Activity Leader and the 2nd Reviewer and leave 2 weeks for feedback and final changes before the due date. Once validated by the 2 reviewers, the draft is ready to be sent to the Management Team that will ask for the Coordinator validation and then transfer it to the EC.*

Annex 2

```
<parameters>
  <!-- ****************************************** -->
  <!-- Simulation scenario parameters -->
  <!-- AquaExcel experiment at Nofima -->
  <!-- Time unit: seconds -->
  <!-- Weight unit: g -->
  <!-- Length unit: m -->
  <!-- Speed unit: m s-1 -->
  <!-- Experimental period -->
  <parameter name="startDate" value="2012.05.11"/>
  <parameter name="endDate" value="2012.10.06"/>
  <!-- Cage/tank dimensions -->
  <parameter name="prodUnitType" value="Tank"/>
  <parameter name="prodUnitShape" value="Circular"/>
  <parameter name="prodUnitDepth" value="2.68"/>
  <parameter name="prodUnitRadius" value="3.5"/>
- <parameter name="prodUnitCentre" type="array">
    <element number="0" value="0.0"/>
    <element number="1" value="0.0"/>
  </parameter>
  <!-- Pellet model settings -->
  <parameter name="pelletModelResolution" value="0.25"/>
  <parameter name="pelletWeight" value="0.03"/>
  <parameter name="pelletSinkingSpeed" value="0.05"/>
  <parameter name="feedInputFormat" value="ReadFromFile"/>
- <parameter name="pulsedFeeding" type="array">
    <element number="0" value="15.0"/>
    <element number="1" value="45.0"/>
  </parameter>
  <parameter name="feederAngle" value="90.0"/>
  <parameter name="feederAirSpeed" value="2.0"/>
  <!-- Environment settings -->
  <parameter name="environmentDataSelector" value="AquaExcel"/>
  <parameter name="envScenarioName" value="nofima_4_7m"/>
  <parameter name="numArtificialLights" value="0"/>
  <!-- Fish settings -->
  <parameter name="fishSizeFormat" value="Weight"/>
  <parameter name="meanBodyWeight" value="83.99"/>
  <parameter name="stDevBodyWeight" value="0.58"/>
  <parameter name="populationSize" value="3863"/>
</parameters>
```

Annex 3

Deliverable D8.1.